Potential of Hybrid Powertrains in a Variable Compression Ratio Downsized Turbocharged VVA Spark Ignition Engine

Energy
Volume 195, 15 March 2020, 117039
https://doi.org/10.1016/j.energy.2020.117039

Antonio García[a], Javier Monsalve-Serrano[a]*, Santiago Martínez-Boggio[a] and Karsten Wittek[b]

[a]CMT - Motores Térmicos, Universitat Politècnica de València, Camino de Vera s/n, 46022 Valencia, Spain
[b]Mechanical Engineering Department, Heilbronn University, Germany

Corresponding author (*):
Dr. Javier Monsalve-Serrano (jamonse1@mot.upv.es)
Phone: +34 963876559
Fax: +34 963876559

Abstract

After the diesel emissions scandal, also known as Dieselgate, Direct Injection Spark-Ignited (DISI) internal combustion engines (ICE) appears as the most promising alternative to mitigate the harmful tailpipe emissions from passenger cars. In spite of that, the current ICE technologies are not enough to achieve the fuel consumption/CO_2 emissions targets set by the new transportation legislation (4.1 $L_{gasoline}$/100km, 95 g_{CO_2}/km for 2021). In this complex scenario, the electrification of the powertrain using high efficiency electric motors and battery package together with sophisticated DISI engines appears as potential solution to meet these requirements. The aim of this work is to study the fuel consumption and pollutant emissions in transient conditions from a passenger car equipped with a variable compression ratio (VCR) DISI engine and electrified powertrain technologies. The vehicle behavior was simulated by means of a 0D GT-Suite model fed by experimental results obtained in an engine test bench. Mild hybrid electric vehicle (MHEV) and full hybrid electric vehicle (FHEV) architectures using a VCR DISI engine were studied. Moreover, an optimization methodology is presented to select the best vehicle configuration in terms of hardware and control strategies by means of a design of experiments (DoE). The results show that VCR allows a fuel improvement of 3% with respect to the conventional DISI fixed CR along the worldwide harmonized light vehicles test cycles (WLTC). The benefits found when combining the VCR technology with hybrid powertrains are even higher. In this sense, the fuel improvements were higher as the electrification levels increased, with 8% for MHEV-VCR and around 20% for FHEV-VCR. In terms of emissions, the two clear benefits with FHEV-VCR were the reduction of particle number (PN) and unburned hydrocarbons (HC) of around 60% and 15%, respectively, as compared to the conventional DISI.

Keywords
Hybrid powertrain; Downsized Combustion Engines; Variable Compression Ratio, Emissions regulations; Driving cycles

1. Introduction

Two-thirds of the oil consumption in the world are currently used in the transportation sector and half of that goes to passenger cars and light trucks [1]. Specifically, the transportation sector accounts for around 25% of the total GHG emissions in Europe. By this reason, the European Commission added targets in terms of CO_2 to the already limits in terms of other pollutants as NOx, Soot, CO and HC. The main challenge proposed to the vehicle manufacturers is to decrease by 35% in 2025 and 67% in 2050 [2]. Therefore, more efficient ICEs working in complex powertrains will play a critical role in meeting such stringent requirements from the cost-effectiveness perspective.

Concerning the current technologies in internal combustion engines, it is well known that conventional compression ignition (CI) engines are noteworthy for transportation vehicles due to their higher efficiency [4]. However, the CI engines require an expensive and complex aftertreatment system (ATS) to control the particulate matter (PM) and NOx control [5,6]. Therefore, the CI engines are preferred in trucks and sport utility vehicles in the last years due to the higher cost of the engine and ATS. Therefore, passenger vehicle manufacturers show a clear preference in the application of DISI engines [7]. In a medium-term scenario, hybrid powertrain combined with downsized SI engines represent the current trend in the vehicle technology to reduce fuel consumption and CO_2 emission [8]. Concerning the ICE downsizing concept, to maintain a reasonable power level in small engines, the application of turbocharging is mandatory [9]. In terms of powertrain electrification, the SI engines have been already integrated in MHEV, FHEV and PHEV [10]. Advanced ICE combustion modes were integrated in electrified powertrains as well trying to obtain more fuel consumption benefits [11]. For example, Atkinson SI engines are popular in the market as the Toyota Prius and Honda Accord with fuel economy improvement of 12% with respect to a conventional SI [12]. Also, low temperature (LTC) combustion as homogeneous charge compression ignition (HCCI) with full hybrid powertrain was also tested in some laboratory prototypes with fuel consumption benefits of 8.8 % in US driving cycles [13]. Advanced SI-ICE controls as cylinder deactivation also show improvements in hybrid powertrains with benefits around 1.5 % in US driving cycles [8].

In spite of these new ICE technologies, other research topic that has received a great interest in the past few years is the right selection of the compression ratio (CR) in SI engines. This selection represents a compromise between low end torque and part load efficiency. In boosted downsized engines, this selection is more restrictive due to the knock phenomenon at high loads [14]. Therefore, a reduction of the CR needs to be done with large fuel penalties [15]. The majority of the boosted engines are equipped with direct fuel injection system and use a CR of approximately 9.6:1 for RON 95 gasoline. The naturally aspirated engines have a higher compression ratio in the order of 10.5:1 to 11:1. The part load efficiencies are also reduced when the boost pressure levels increase [16]. Therefore, several research groups and companies are studying the variable compression ratio (VCR) system as a way to overtake this problem [17,18]. An assessment of the different technological ways to modified constantly the CR in an ICE can be found in [16]. The study of Wittek et al. [18] using a variable connecting road with a high CR of 12.1:1 and a low CR of 9.6:1 moved by a hydraulic system in a 1.0 L boosted engine reports fuel consumption improvements up to 5% at stationary conditions of low and medium loads with high CR, and operability up to 26 bar with low CR. Kleeberg et

al. [19] estimated the fuel consumption by vehicle simulations in a 2.0 L DISI VCR engine with a conventional powertrain (no-hybrid) in US driving cycles. A mapped based approach was used, reporting improvement of 5–7% with market gasoline. In addition, ethanol and CNG were found to be suitable fuels to achieve higher engine thermal efficiencies and lower CO_2 emissions due to the lower C/H ratio. Teodosio et al. [20] also reported vehicle fuel consumption by a 0D vehicle mapped based method in a twin-cylinder PFI SI VCR 0.9 lt engine. The WLTC was used with a no-hybrid vehicle. Fuel benefits of 1.7% were reported.

In spite of existing several works using VCR systems in single and multi-cylinder engines, a few works have studied the benefits in transient conditions and none in hybrid powertrains architectures. Considering this, the aim of this study is to identify the potential benefits in terms of fuel consumption and emissions of using a VCR downsized ICE in full hybrid electric powertrains. Thus, a DISI 1.0L three cylinder boosted engine with variable valve actuation (VVA) and VCR technology was used in several hybrid powertrain layouts. Therefore, the combustion propeller used in this work has the most innovative technology in SI ICE field. Combining these two technologies, which are not commercially found at large scale, it is expected to have a perspective of the next generation of commercial passenger vehicles. A numerical model fed with experimental ICE test bench results is used to account the fuel consumption and emissions in the Worldwide harmonized light vehicles test procedure (WLTP) for a B-segment passenger car. This means the test in two driving cycles: the worldwide harmonized light vehicles test cycle (WLTC) and a real driving cycle (RDE) measured by the authors.

2. Materials and methods

The evaluation of different hybrid powertrains in a DISI three cylinder boosted VCR engine was performed in a numerical 0-D vehicle model. Dedicated modules are added to model the driver behavior (driving cycle speed traces) and vehicle components (transmission, differential, wheels among others). Lastly, the electric components as the battery package and motors are added with dedicated efficiency maps.

The main input of the model is the ICE calibration maps for fuel consumption and engine-out emissions (CO_2, CO, HC, NOx and PN) performed experimentally. This approach is usually called as map-based vehicle simulation and only takes into consideration the system dynamics by means of a quasi-steady modeling. Therefore, even though the fuel consumptions and emissions are calculated as a function of the dynamic ICE speed and load profiles, each instantaneous condition is based on experimentally-derived stationary maps. In spite of the simplicity of the ICE model, it was extensively used in the research field to estimate the vehicle performance, fuel consumption and emissions due to the acceptable accuracy and low computational cost [21]. Vassallo et al. [22] reported fuel consumption and NOx engine-out emissions differences between 3% and 8%, respectively, in a turbocharged diesel engine by comparing dynamic engine test bench results. In a previous work [23], the authors of the current work showed differences between experiments and simulations in a diesel Euro 6d-temp with parallel full hybrid technology of 3% and 4% for fuel consumption and emissions, respectively. Pasquier et al. [24] reported a fuel consumption deviation between 0.6% and 1.5 % depending on the driving cycle for a SI engine. In general terms, the estimations are acceptable in homologation driving cycles at warm conditions, in which the engine load changes gradually.

This section is divided into two subsections. First, the experimental campaign to obtain the stationary engine maps is explained. Later, the details of the vehicle and numerical model are provided.

2.1. Engine and test cell

The first step to study the vehicle behavior in transient conditions is to measure the ICE behavior at stationary and warm conditions. These results are used to estimate the fuel consumption and emissions in transient conditions. As the engine processes are complex (combustion, air management, among others), this approach leads to acceptable estimation in terms of fuel consumption and emissions. Several authors used this approach with total errors below 5% [25,26]. The errors for this model during the warm-up phase of the engine are higher of 15% [22] due to the difference between the stationary warm map and the transient real engine temperature. Therefore, in this work it was preferred to model the vehicle performance at warm conditions (liquid coolant temperature at 80°C and oil temperature at 90°C).

The internal combustion engine used in this work is a turbocharged 3-cylinder DISI equipped with a prototype 2-stage VCR-system developed by Heilbronn University. The basis of the engine tested is a commercial original equipment manufacturer (OEM) Ford EcoBoost production 1.0 L engine generally equipped in the models Fiesta, Focus, Mondeo and C-max, among others. The engine architecture features a four-valve pent roof combustion chamber with a central mounted DI injector, an integrated exhaust manifold, double cam phasers and a waste-gate turbocharger. Oil pressure is generated by a switchable variable vane oil pump which can be run at two target pressure (relative) set points of 200 kPa and 400 kPa. The main engine parameters can be seen in Table 1 and in previous works [18].

Table 1- VCR DISI engine characteristics.

Parameter	Value
Engine Type	4 stroke, 4 valves, direct injection, spark ignited
Number of cylinders	3
Stroke	82 mm
Bore	72 mm
High CR	12.11
Low CR	9.56
Connecting Rod variation in length	2.2 mm
Total mass connecting rod assembly	660 g (OEM 415g)
Maximum Power tested	73 kW @ 4000rpm

In spite of the maximum power output tested was measured at 4000 rpm, the OEM engine achieved 88 kW at 6000 rpm. As it is not necessary the measurements of this engine zone for the analysis of the performance in typical homologation cycles, the maximum ICE speed tested was 4000 rpm. The engine management was done with a free programmable ECU (Schaeffler, type PROtroniC) featuring all the needed driver stages and software functions such as closed loop control for lambda, throttle position and boost pressure. More details of the experimental set up are described in [18].

A commercial gasoline (RON 95) was used in the experimental test (see Table 2). The injection duration was closed loop controlled, targeting a stoichiometric air equivalence

ratio, i.e., λ=1 in the entire operating range. The ECU set values were re-adjusted to achieve high efficiency operation. On the other hand, for a comparative purpose between the VCR and fixed compression ratios, the valve timing, injection timing and injection pressure were maintained to take in account only the effect of the compression ratio variation. Therefore, the ignition angle was set manually, targeting the center of combustion (CA50MFB) to occur at 8 CAD ATDC, when possible. For extreme operative conditions, the maximum retard in SA was fixed at 30 CAD ATDC to not elevate the exhaust gas temperature above the turbine and catalyst limit (around 950°C). Also, the maximum allowed peak firing pressure of 12 MPa was used for mechanical limitations.

Table 2 – Gasoline main properties used in the experimental and numerical test for fuel the ICE.

Fuel Properties	Value
LHV [MJ/kg]	42.55
$Density_{@15ºC}$ [kg/m^3]	739.9
$AFR_{stoichiometric}$	14.21
Carbon ratio [%]	83.79

The engine test bench with the control and measurement system is shown in Figure 1a. The VCR conrod design is shown in Figure 1b. With this VCR connecting rod two effective lengths and thus two different CRs can be adjusted. The low CR (9.56:1) when the system is in the lowest position and high CR (12.11:1) when the support moves upward. The piston pin is supported in an eccentric. The effective length of the connecting rod is varied through an angular travel of this eccentric. The eccentric is kept in a desired end position by means of a support mechanism consisting of two hydraulic cylinders. Further explanations on the working principle of the VCR connecting rod and its actuation can be found in [18].

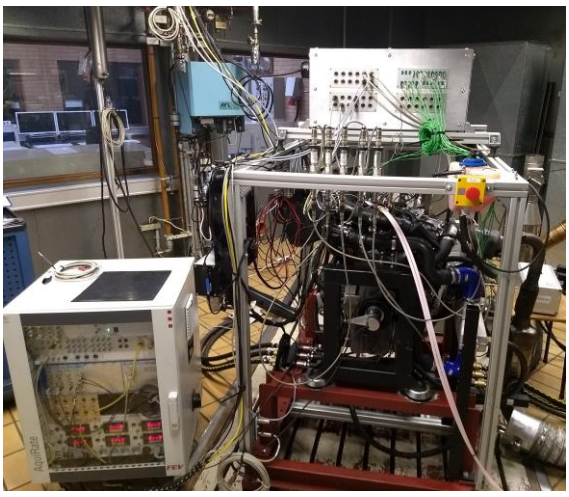

(a)

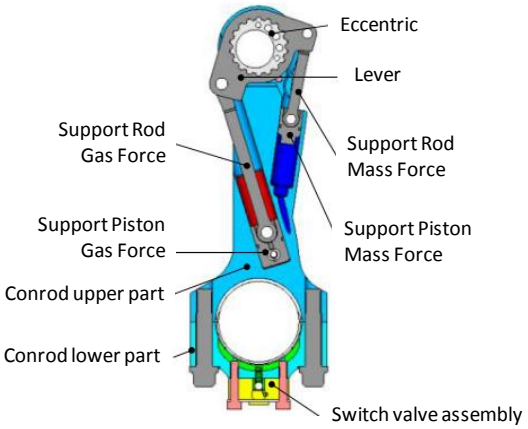

(b)

Figure 1 – Engine test bed with the 1.0 lt Boosted VCR engine (a) and the connecting rod scheme for VCR system.

The fuel consumption engine maps for low and high CR are presented in

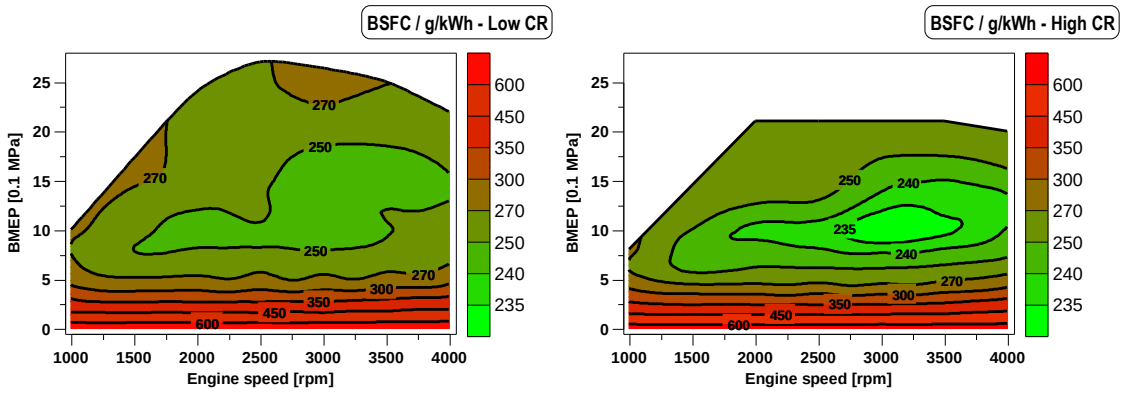

(a) (b)

Figure 2. It is important to note that each engine map contains 70 stationary points with measurements of fuel consumption, CO_2, NOx, HC, CO and PN emissions. All the measurements are performed with the VCR connecting rod system in the two possible positions. Later, an optimum map was performed by joining both maps with the target to achieve the minimum fuel consumption (Figure 3). The fuel improvements with high CR at low load (below 10 bar) are between 4% and 5%. The optimum BSFC switch line (dashed line in Figure 3) marks the best strategy to change the CR to obtain fuel gains. Figure 4 shows the brake specific NOx (BSNOx) emissions and brake specific particle number (BSPN) for the combined CR selection at engine-out conditions (before ATS). The CR decrease at high load allows to better control the NOx emissions. The maximum level of this pollutant is achieved at the highest load of the high CR (below the dashed line in Figure 4a). The particle number does not show a high variation with the CR change, being the transition smooth between both CR (see Figure 4b). This information could help researchers and engine manufacturers for future engine calibration and emissions estimations. The other emissions maps are presented in the Appendix A (Figure A1 and Figure A2) for the brevity of the manuscript. More information about the engine test campaign is detailed in [18].

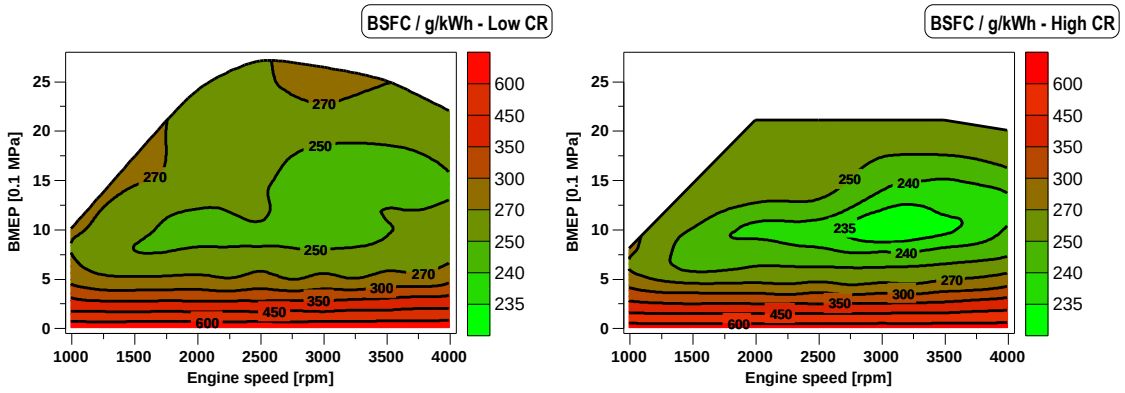

(a) (b)

Figure 2 – Brake specific fuel consumption at low (a) and high CR (b).

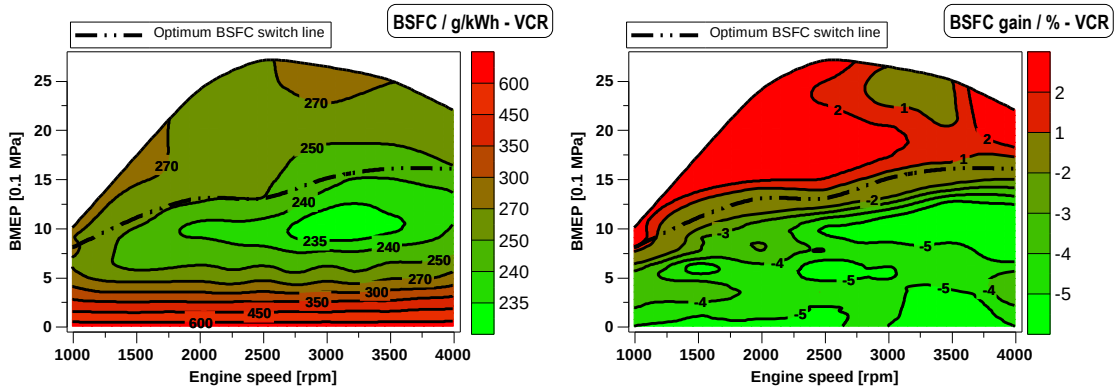

(a) (b)

Figure 3 – Optimum brake specific fuel consumption for each operating condition combined the right CR selection (a) and the fuel improvements map with respect to the low fix CR (b).

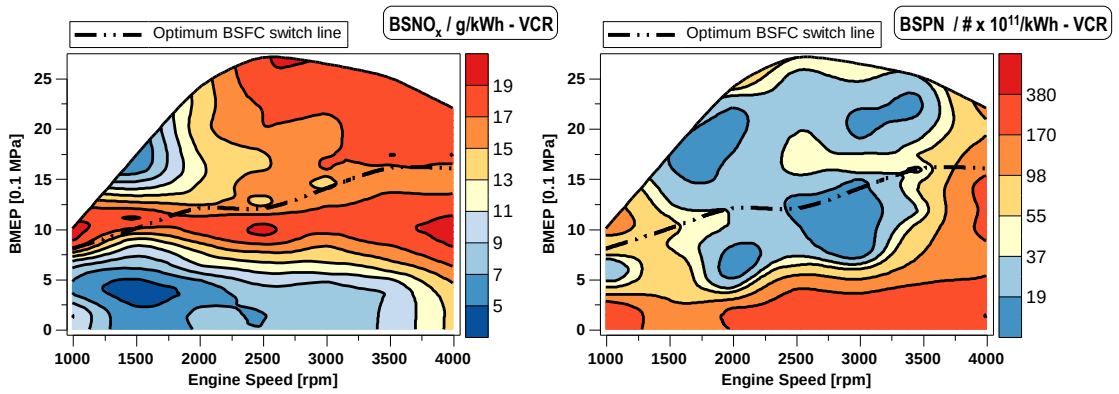

(a) (b)

Figure 4 – VCR brake specific NOx (a) and Particle number (b) engine-out emissions.

2.2. Vehicle, computational model and validation

2.2.1. Vehicle Specifications and Numerical Models

The vehicle selected to perform the simulation is a subcompact (Class B) passenger car Ford Fiesta, which equips the DISI EcoBoost engine used in the experimental test bench. The main parameters of the vehicle and the Heilbronn University test vehicle are described in Table 3. This vehicle has a conventional powertrain architecture (no-hybrid) with the ICE coupled to a manual 5-gear transmission by a clutch. The final coupling is done by the differential with the front wheels.

Table 3 – VCR vehicle demonstrator specifications.

Vehicle type [-]	OEM
Base vehicle Mass [kg]	1016
Passenger and Cargo Mass [kg]	100
Fuel Mass [kg]	45
Vehicle Drag Coefficient [-]	0.328
Frontal Area [m²]	2.14
Tires Size [mm/%/inch]	195/55/R15
Gear Ratios [-]	3.6/1.9/1.2/0.9/0.7
Differential ratio [-]	3.61

The GT-suite (v2019, Gamma Technologies, LLC., Westmont, IL, USA) 0D vehicle model was used to analyze the vehicle performance under several powertrain architectures and driving cycles. An in-house rule-based control (RBC) system specially designed to perform transient operation under hybrid and no-hybrid vehicles platforms was used (see Appendix B). This system controls the split between the ICE and EM as well as the different vehicles modes as: regenerative braking, battery charging, power assist and pure electric mode. Dedicated modules are used to simulate the behavior of the different components as EM, battery, transmission, wheels among others. Specifically, the transient simulation model consists of a driver sub-model trying to follow a predetermined speed profile used as input. Therefore, the desired torque is calculated by the vehicle traction equations considering the road friction and aerodynamic forces, among others [27].

In this work, four hybrid architectures were tested with the engine maps of the VCR. MHEV-P0, FHEV-P2, FHEV-Series and FHEV-Series Parallel were tested. These architectures are the most representative of the current commercial powertrain layout, in which the main difference is the battery capacity as well as the EM position and maximum power output. As the name suggest, mild hybrid is a first step towards the conventional powertrain and BEV. It integrates a battery of low capacity (<2kWh) and medium-term voltage (<60V) [28]. In addition, the denomination of P0 is due to the position of the EM in the engine platform replacing the traditional alternator. The main capabilities of this type of layout are the start-stop function avoiding the idle consumption in urban areas, the power assist of the ICE and the regenerative braking [29]. A scheme of the powertrain is depicted in Figure 5a. The advantages are the low complexity of the system, so can be easily coupled to the actual vehicle designs, and the reduce in development and hardware cost with respect to a FHEV or BEV. On the other hand, the main limitation is not having a pure electric mode. Thus, it never operates at zero tailpipe emissions.

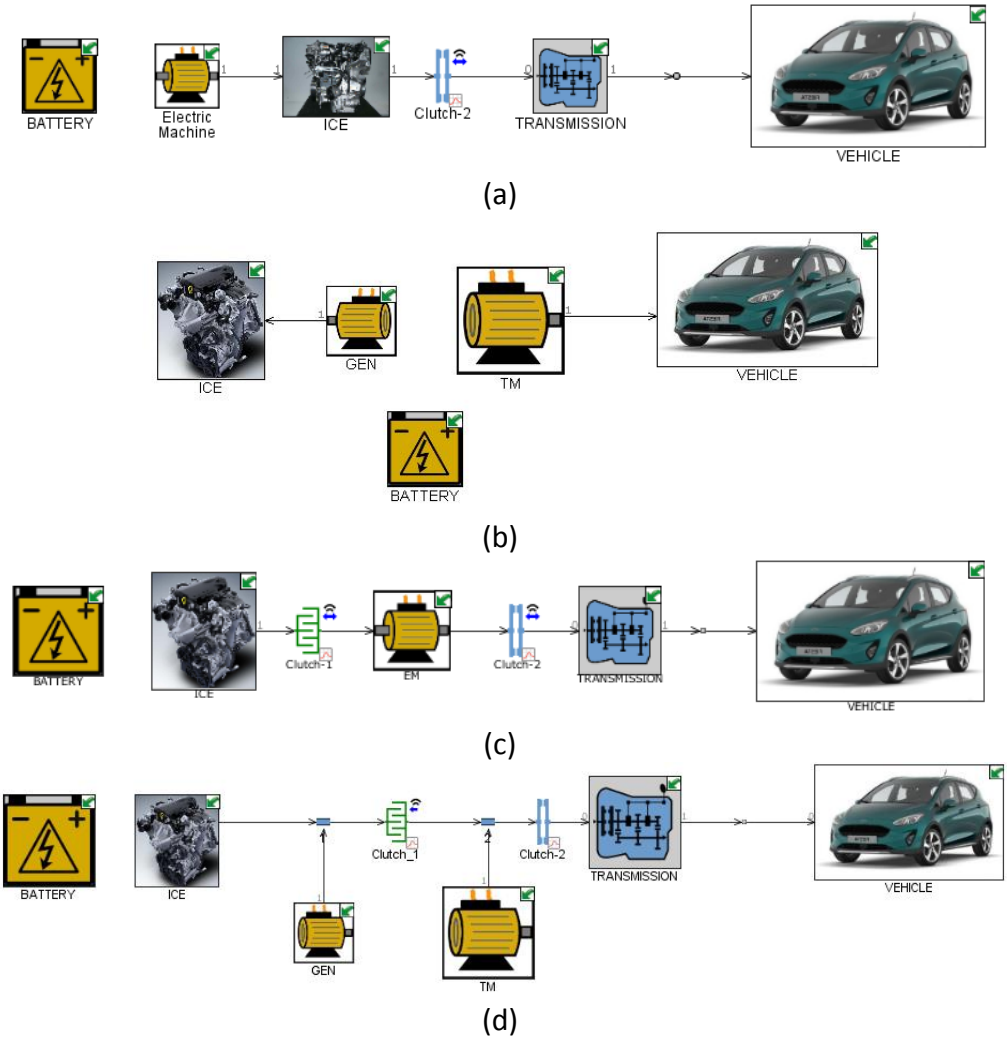

Figure 5 – Powertrain layout for the Ford Fiesta VCR hybrid vehicle: MHEV-P0 (a), FHEV-Series (b), FHEV-P2 (c) and FHEV-Series Parallel (d) .

The next step in electrification level are the FHEV vehicle with the series (Figure 5b), P2 or parallel (Figure 5c) and the series parallel (Figure 5d). The common characteristic between them are the battery capacity (2kWh<Batt<15kWh) and voltage (>300V) as well as electric motor capable to propel the vehicle even at high vehicle speed (>80 km/h) [30]. In detail, the series also called range extender separates the ICE from the drivetrain. Therefore, the main advantage is the capacity to set the desired ICE rotational speed and load independent of the requirement of the driving cycle. Generally, this architecture uses a limited range of the ICE map in the zone of minimum fuel consumption. The Traction Motor (TM) always propels the vehicle and the generator motor (GEN) set a load in the ICE when the battery achieves a certain state of charge (SOC). For this study, three stationary points were used, depending on the SOC value, selected over the line of minimum fuel consumption.

The P2 FHEV technology is an upgrade of the P0 MHEV due to the installation of an EM between the ICE and the transmission. Thanks to a double clutch system, this hybrid architecture allows the operation as pure BEV (clutch 1 disengaged) and in power assist mode (clutch 1 engaged). Also, regenerative braking and battery charging are the other available modes. The main restriction of this architecture is the ICE operative rotational speed that only could be changed by the transmission ratios and not set freely. However,

the high capability of the power assist mode and the simplicity of the EM location, positioned this architecture as one of the most used in the automotive industry [31]. In order to take the advantages of the last two technologies, it was designed the series-parallel FHEV architecture (see Figure 5d). Instead of using one EM as P2, a GEN and TM are included separated by a clutch (clutch-1). Therefore, with this system disengaged the vehicle operates as a series, while it operates as parallel when the system is engaged (P2). One of the main disadvantages of this technology is the high complexity and the number of additional components that need to be added in the driveline and control system. A resume of the different control parameters for each powertrain architecture is detailed in the Appendix B (Table B1 and Table B2).

As it can be seen, each technology has advantages and disadvantages in terms of operability and complexity. Several authors affirm that it not exists a universal best approach and the main parameters that determine their selection are the vehicle manufacturing requirements and ICE performance [32]. For this reason, in this study it was set that all the hybrid technologies need at least the same power output than the OEM Ford Fiesta EcoBoost vehicle (88 kW).

2.2.2. Driving Cycles and Optimization Methodology

The WLTP was developed with the aim of being used as a global test cycle across different worldwide regions, so that the pollutant and CO_2 emissions as well as fuel consumption values would be comparable worldwide. In addition, traffic and weather conditions will also add variations between lab conditions and the real world. Therefore, the new European emissions legislation adds to the initial WLTC (Figure 6a) the real driving emissions (RDE), in which pollutant emissions are measured during the real vehicle operation on the road [35]. As it is expected that RDE conditions has higher emissions values than WLTC, the EU commission determines conformity factors of 1.43 for NOx and 1.5 for PN with respect to WLTC Euro 6 limits until 2025. This conformity factors are also necessary to consider that the accuracy of the portable emissions measurement systems (PMES) is not as high as that of the laboratory equipment. To make the study closer to the current regulation, an in-house RDE cycle was measured in Valencia-Spain (Figure 6b) with the aim to evaluate the results in the both types of WLTP cycles (WLTC + RDE) [36].

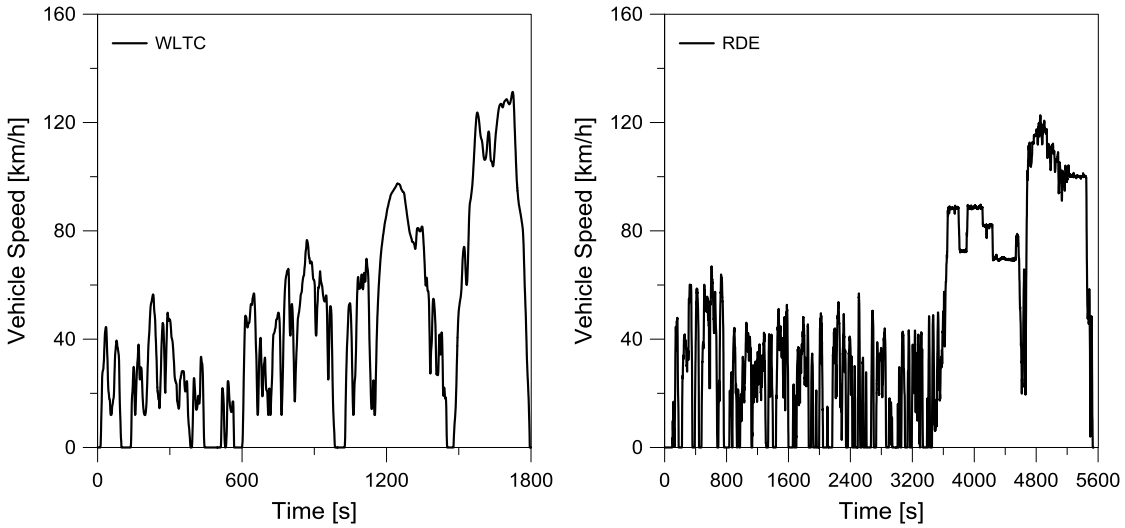

Figure 6 – WLTP driving cycles with the laboratory pre-defined WLTC (a) and in-house measured RDE (b).

The optimization of the different powertrains is performed with a design of experiments (DoE) in which 800 different cases varying the hardware capacity and the control strategies are tested. The distribution of the cases was done by means of a Latin hypercube sampling due to the near-random sample of the parameter values from multidimensional distribution [37]. The DoE is performed in the WLTC because is the unique pre-established cycle of the current normative. A summary of the DoE parameters and range tested are showed in Table 4. After that, the optimum selected cases for each powertrain layout are tested along the RDE cycle to better understand the vehicle performance in real-world conditions.

Table 4 – DoE parameters to study the best components and control selection for each powertrain architecture.

Powertrain	Parameter	Range
No-hybrid	Gear shift [rpm]	1000-4000
P0-MHEV	Gear shift [rpm]	1000-4000
	Battery Capacity [kWh]	0.5-2.0
	Electric Motor Max Power [kW]	8-20
	Split ICE-EM [%]	0-100
Series-FHEV	Battery Capacity [kWh]	2.0-12.0
	Generator Motor Max Power [kW]	30-90
	Differential Ratio [-]	2.0-6.0
P2-FHEV	Gear shift [rpm]	1000-4000
	Battery Capacity [kWh]	2.0-12.0
	Electric Motor Max Power [kW]	25-50
	Split ICE-EM [%]	0-100
	Maximum speed BEV mode [km/h]	25-140
Series Parallel-FHEV	Gear shift [rpm]	1000-4000
	Battery Capacity [kWh]	2.0-12.0
	Traction Motor Max Power [kW]	20-60
	Generator Motor Max Power [kW]	5-50
	Split ICE-EM in parallel mode [%]	0-100
	Maximum speed Series mode [km/h]	25-140

3. Results and discussion

The results are divided into three subsections. The first subsection shows the DoE results for the different vehicle architectures. Due to the similarities, P0 MHEV and P2 FHEV are showed in a first part and Series and Series-Parallel FHEV are analyzed later. The optimum case is selected for each architecture. Therefore, in a second subsection, a deep comparison between the optimum cases and the advantages and disadvantages of each architecture is carried out. Lastly, the optimum vehicle platforms are also evaluated in an RDE cycle. In all the sections, the no-hybrid VCR and the no-hybrid fixed CR vehicle (conventional DISI) are used as reference.

3.1.1. Powertrain Optimization

3.1.1.1. Mild and P2 Hybrid Electric

Figure 7a show the engine-out NOx emission against the fuel consumption along the WLTC. The NOx trend for the hybrid and no-hybrid shows a decrease with the reduction of fuel consumption. This is mainly due to the engine map calibration for both CR instead of the electrification. Figure 4 shows that the NOx levels decrease with the load and with the engine speed. Therefore, setting a shift strategy to promote using engine speeds below 2000 rpm will reduce the NOx emissions. In addition, the increase in the powertrain electric capacity coupled with the VCR system allows a strong decrease of the fuel consumption. In spite of this improvement, the Euro 6 limits (0.06 g_{NOx}/km) are far of the engine-out levels obtained. Therefore, an aftertreatment device must be used in these platforms to reduce the NOx. Generally, a three-way catalytic (TWC) is used due to the high conversion efficiency and reduced cost. A discussion about the ATS system needed for the different vehicles is included in the next section.

As it is well known, DISI engines have serious problem with soot emissions due to the fuel impingements and pool fires inside the combustion chamber. Although, this engine calibration was performed with a homogeneous injection strategy with an early injection timing, the particulate number is high. Figure 7b shows that fixed CR and VCR no-hybrid have similar values in terms of PN, all over $8x10^{11}$ #/km. On the other hand, the hybridization of the powertrain allows to decrease the PN with P2 FHEV inside the Euro 6 limit (marked with a dashed rectangle, $6x10^{11}$ #/km). This is an advantage of the hybrid powertrains due to reduction of the ATS complexity. In particular, the gasoline particle filter (GPF) could be removed ideally.

The HC and CO emissions are depicted in Figure 8. The VCR engine operation increases the HC emissions with respect to the fixed CR from 0.6 g/km to 0.8 g/km approximately (Figure 8a). On the other hand, the electrification of the powertrain allows to decrease the HC emissions to values below the fixed CR no-hybrid for P2 FHEV and close to the P0 MHEV. In the case of CO (Figure 8b), the emission levels are similar for the different vehicle platforms. All the cases present a parabolic behavior with the minimum CO emission at high fuel consumption. This is mainly because of the gear shift strategy, since it is the unique common parameter between all the vehicles. Only a slight CO decrease is seen for the P2 FHEV. For all the cases, the three-way catalyst is necessary to achieve Euro 6 limits (marked in dash rectangle) in HC (0.1 g_{HC}/km) and CO (1.0 g_{CO}/km) emissions.

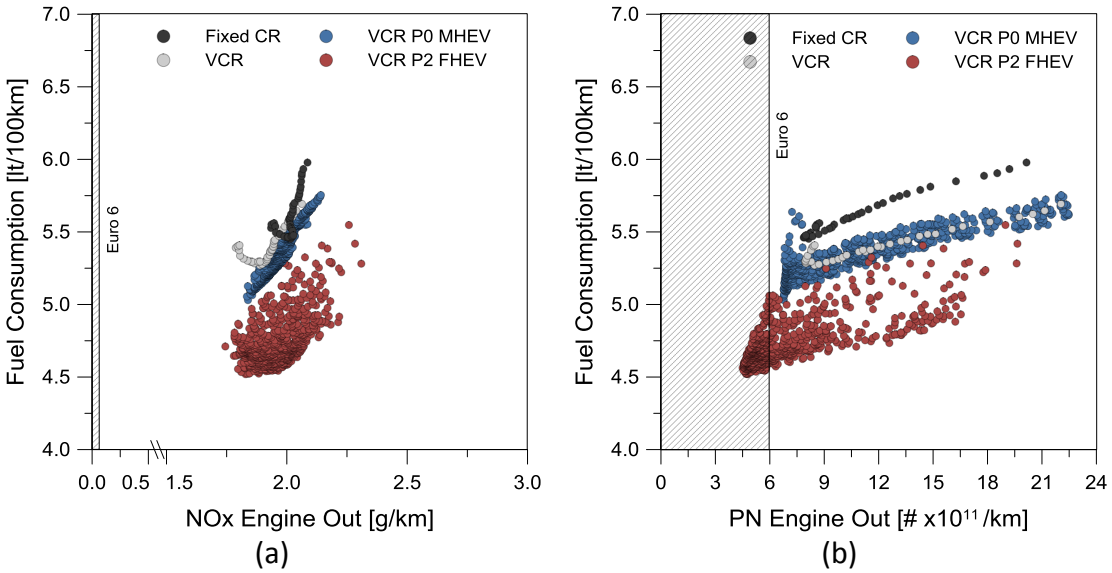

Figure 7 – Fuel consumption against NOx (a) and particulate number (b) at engine-out for the different DoE cases in MHEV and P2 FHEV powertrains with VCR. No-hybrid VCR and fixed CR are presented for comparison.

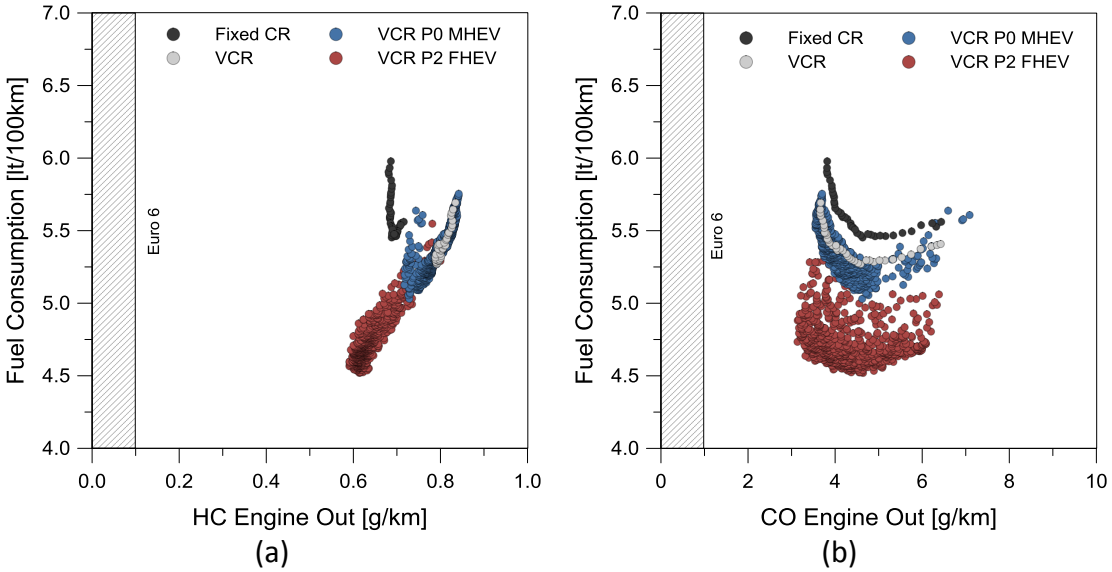

Figure 8 – Fuel consumption against HC (a) and CO (b) at engine-out for the different DoE cases in MHEV and P2 FHEV powertrains with VCR. No-hybrid VCR and fixed CR are presented for comparison.

The main results from the previous results is the possibility to reduce the fuel consumption without high penalties in NOx and Soot emissions (see Figure 7) in the hybrid powertrains. Also, there is not a high increase in HC and CO in the minimum fuel consumption case. Therefore, the vehicle configuration that allows the minimum fuel consumption was selected as optimum case. In spite of the trends showed before are important, it is necessary to understand which parameters are those that affect the fuel consumption results for each vehicle platform. Figure 9 shows the battery capacity and electric motor maximum power effect in the fuel consumption. The P0 MHEV shows a decrease trend in the fuel consumption with the reduction of the battery size (Figure 9a). This suggest that low battery capacity is necessary due to the low power assist capabilities and the absence of the pure electric mode. Thus, the reduction of the battery capacity implies a decrease of the vehicle weight, improving the fuel consumption (around 5%). On the other hand, the P2 FHEV shows a flat trend between

the fuel consumption with the battery size, the minimum values are closer when comparing the extreme cases (2 kWh and 12 kWh). A medium battery package (5 kWh/400v) shows the minimum fuel value in the WLTC. For both architectures, the EM shows not great influence in the fuel consumption (Figure 9b). The optimum was found closer to the minimum tested in the DoE range.

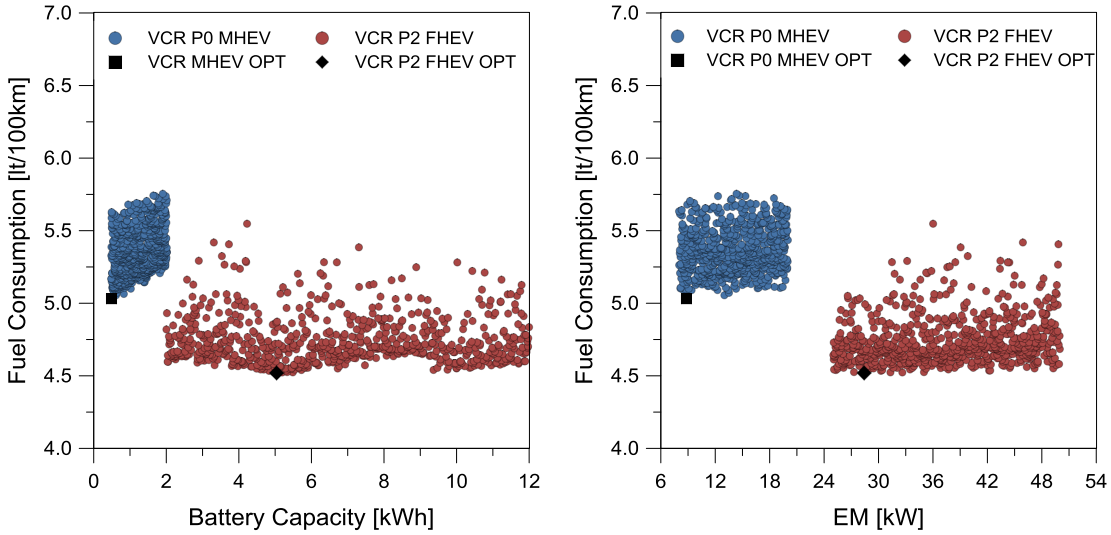

Figure 9 – Fuel consumption against Battery size (a) and Electric Motor maximum power (b) for the different DoE cases in MHEV and P2 FHEV powertrains with VCR.

The power assist mode allows an increase in the power output of both hybrid architectures as well as assisting the ICE at medium and low loads. Figure 10a shows the level of assist that is performed when the battery does not need to be charged and the required torque is enough for that the EM takes part of the propulsion. The results suggest that high level of assistance (around 95%) it is preferred for P0 MHEV and medium level (60%) for P2 FHEV. However, it is not a clear trend between 20%-100% level of assistance. Additionally, to the power assist mode, the P2 FHEV has a pure electric mode in which the EM propel the vehicle on his own. In the control strategy, it was optimized the maximum speed allow to operate in this mode. The idea with this is to not using the EM in high speed and loads in which the ICE is efficient. As the Figure 10b shows, the best speed selection it is at high speed levels (around 70 km/h). However, above 60 km/h it is possible to see similar results to that found at 140 km/h. Therefore, the results suggest that low vehicle load and speed phases are better to use the EM instead the ICE, as was expected due to the higher fuel consumption (see Figure 2).

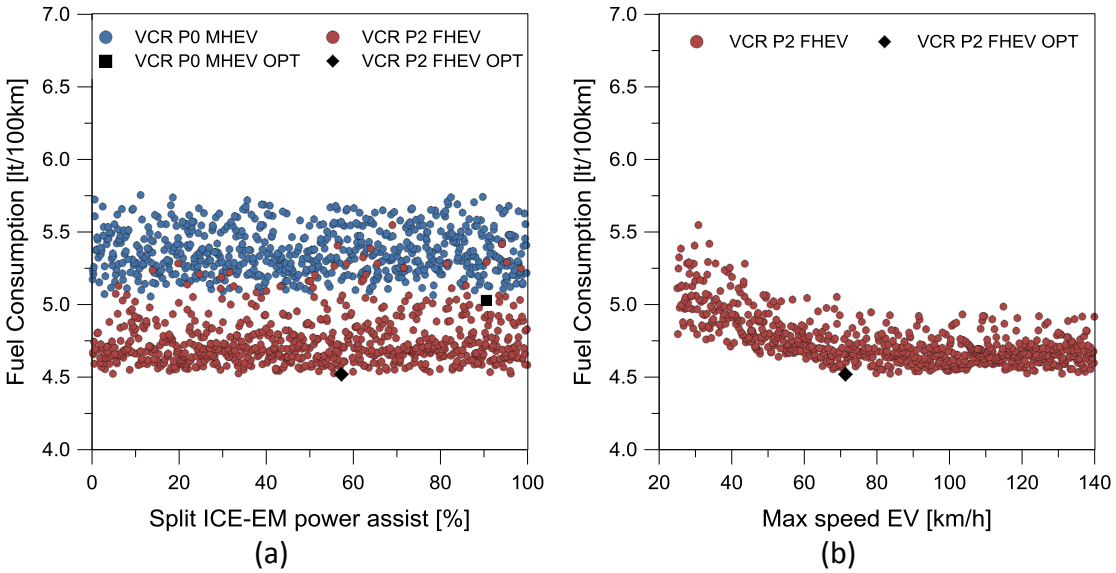

Figure 10 – Fuel consumption against ICE-EM split in power assist mode (a) and maximum vehicle speed at pure electric mode (b) for the different DoE cases in MHEV and P2 FHEV powertrains with VCR.

The only common parameter of these three types of powertrains (no-hybrid, P0 MHEV and P2 FHEV) is the gearbox shifting, which can be tuned to run the engine speed in a desired rotation speed range. The gear strategy was optimized in the driver setup in order to change the engine speed operation. The x-axis of Figure 11 shows the output transmission shaft speed at which a certain gear is changed to the upper one. A gap of 500 rpm was used to make the downshift. The results suggest that the influence of this parameter is stronger than the previous analyzed parameters. The trend seems a parabolic effect with a decrease when reduce the rotational speed shift up to a limit that increase again. For the hybrid vehicles, the optimum point is closer to 2000 rpm. However, for the no-hybrid the optimum engine speed is higher (around 2000 rpm) due to limitations of the power output at this low speed. This difference is because the hybrid powertrains has the advantage of using the power assist mode, which compensates the power required at low engine speed.

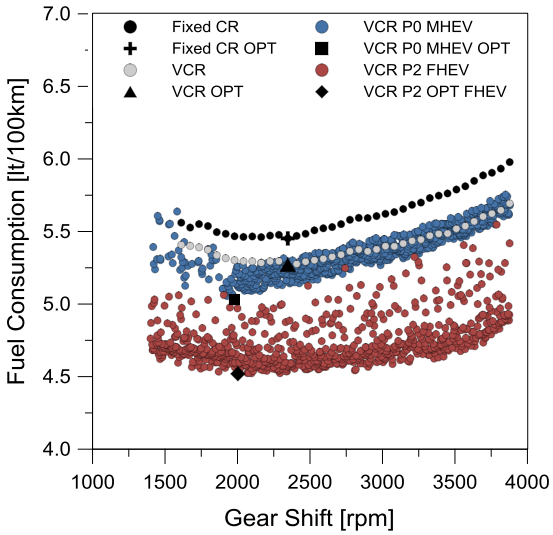

Figure 11 – Fuel consumption against gear shift strategy for the different DoE cases in P2 FHEV powertrain with VCR.

3.1.1.2. Series and Series-Parallel

The other two hybrid architectures tested were the Series and Series-Parallel. Both vehicle platforms have the advantage of being able to disengage the ICE of the wheels. Thus, the engine speed and load could be set as desired during the charge of the batteries. This means to avoid the transient operation, improving the ICE operation and efficiency. The control system was programmed to operate, for each load set, at minimum BSFC when operate at series mode. In spite of the series only operates under this mode, the series parallel have the additional capacity to change to parallel operation depending on the vehicle speed (ICE+EM propel the wheels).

Figure 12a shows the NOx emissions against the fuel consumption for the different vehicle platforms. The hybrid vehicles with series mode allow a strong decrease of the fuel consumption with respect to the no-hybrid vehicles. However, the NOx emissions are increased between 30% and 50%. This behavior is because of the operation closer to the minimum BSFC zone, in which the fuel consumption is highly improved with respect to low load map zone but the NOx emissions are high. Moreover, it is possible to see higher dispersion of the series-parallel cases than the series one due to the change between series and parallel mode. In spite of the higher variability in the output values, it is possible to improve the fuel consumption with the series-parallel architecture due to operating at parallel mode at high speeds. On the other hand, Figure 12b shows the PN emissions, in which both hybrid vehicles have a strong reduction. As was seen for the P2 FHEV, these two FHEV platforms can also achieve Euro 6 PN limits (dashed box).

Figure 13 shows the HC and CO emissions with respect to the fuel consumption in all the series and series-parallel cases tested. This hybrid typology allows to reduce both parameters for most of the cases. This is mainly thanks to the operation near the optimum BSFC in which the combustion efficiency is the highest. The series-parallel has a large reduction of HC when operates at high loads (low HC in Figure A1a of the Appendix A).

Performing a deeper analysis of the results, it was seen that the main parameter that determines the vehicle performance for these hybrid platforms is the generator capacity (Figure 14a). This is due to the link between the operation point and the maximum generator capacity programming in the control system (Table B2 in Appendix B). Figure 14a shows that the higher generator capacity uses only one zone of the engine map. Instead, it is necessary to use three engine zones when the generator capacity is below 40 kW. Figure 14b shows that the battery capacity does not have a great influence on the fuel consumption. Above 3 kWh, the results are closer to those found with a high battery package. The other parameters are not showed for the brevity of the manuscript. However, their influence on the fuel consumption is weak. As was seen for the P0 and P2, the fuel consumption decreases together with the NOx and Soot. Therefore, the optimum configuration for both powertrain platforms was selected at the minimum fuel consumption.

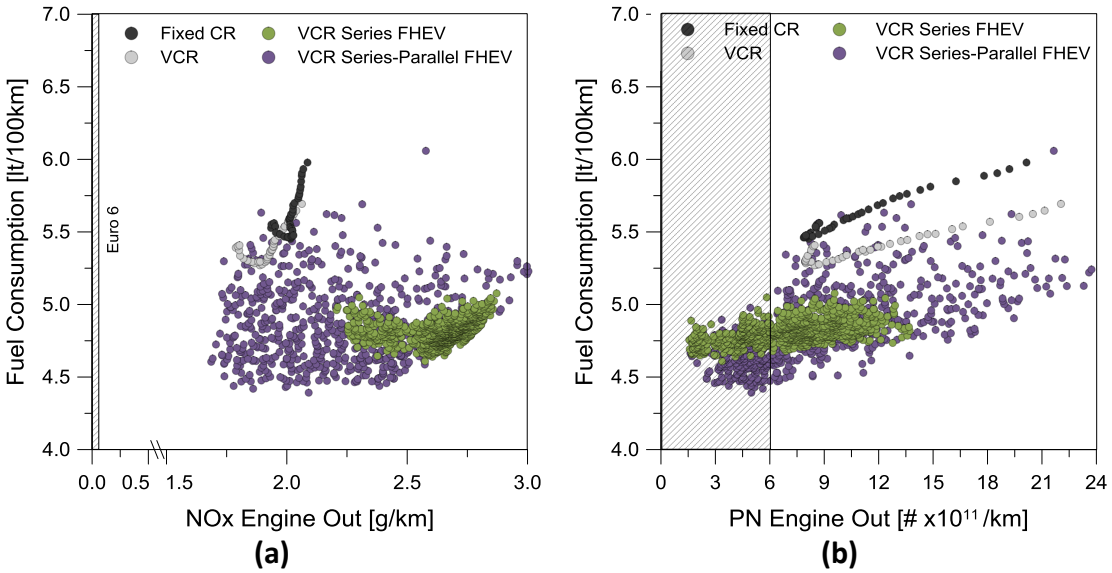

Figure 12 – Fuel consumption against NOx (a) and particulate number (b) at engine-out for the different DoE cases in Series and Series-Parallel FHEV powertrains with VCR. No-hybrid VCR and fixed CR are presented for comparison.

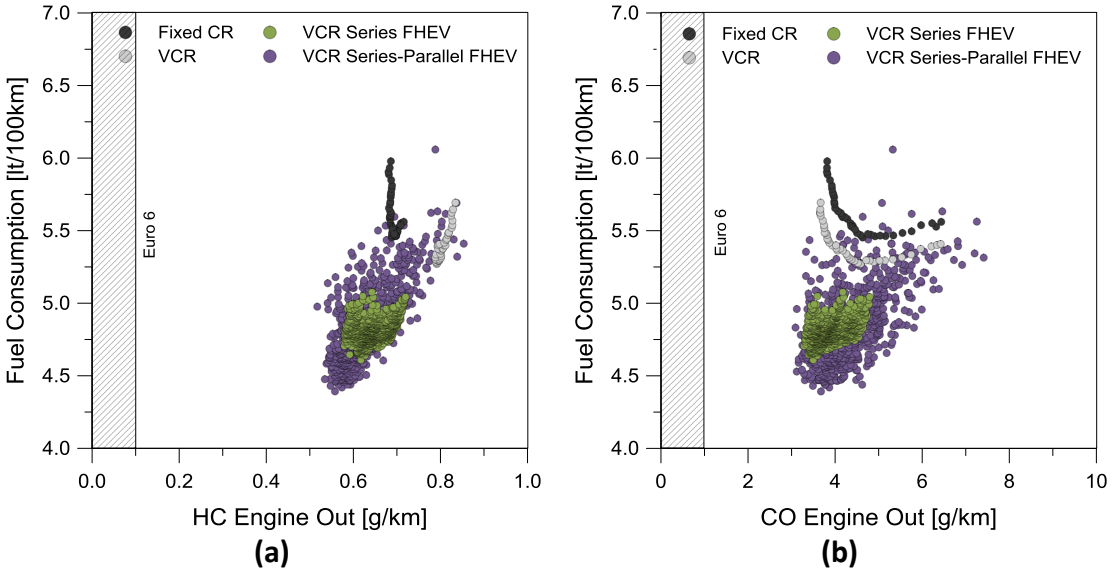

Figure 13 – Fuel consumption against HC (a) and CO (b) at engine-out for the different DoE cases in Series and Series-Parallel FHEV powertrains with VCR. No-hybrid VCR and fixed CR are presented for comparison.

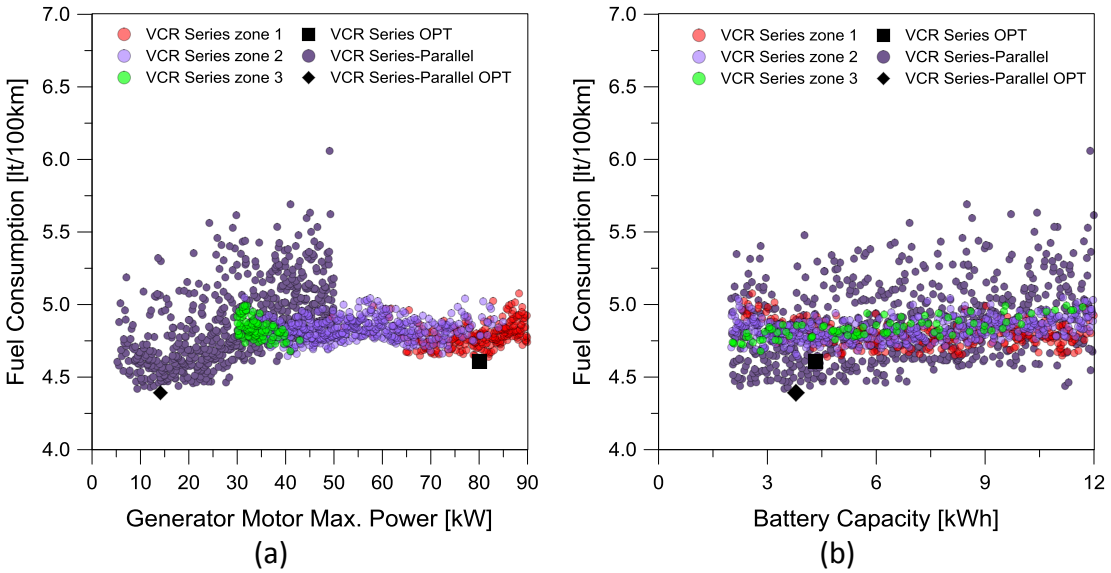

Figure 14 – Fuel consumption against Generator Maximum Power (a) and Battery size (b) for the different DoE cases in Series and Series-Parallel FHEV powertrains with VCR.

3.1.2. Hybrid Powertrain potential under optimal conditions

After the analysis of the results for all the cases tested, this section presents the performance results for the optimum powertrain configuration (hardware + control) in each architecture. Table 5 shows the hardware and control selection for each architecture. The P2 FHEV needs a higher battery package than the other hybrid vehicles due to using the pure electric mode. On the other hand, the total vehicle weight is lower than the series and series-parallel due to the use of a single EM to perform traction and battery charging. The P0 MHEV is the lightest hybrid car with only 40 kg more than the no-hybrid vehicle. In this analysis was considered as hypothesis that the VCR system does not add extra weight to the vehicle.

Table 5 – Optimum components and control selection for each powertrain architecture to achieve the minimum fuel consumption in the WLTC.

Vehicle Platform	Shift Strategy [rpm]	Battery Capacity [kWh]	Traction Motor [kW]	Generator Motor [kW]	Split ICE-EM [%]	Speed Limiter mode [km/h]	Axle ratio [-]	Vehicle Weight [kg]
Fixed CR No-Hybrid	2350	-	-	-	-	-	3.6	1161
VCR No-Hybrid	2350	-	-	-	-	-		1161
VCR P0 MHEV	1980	0.5	9		90	-		1201
VCR Series	-	4.3	88	80	-	-	3.2	1238
VCR P2 FHEV	2000	5.0	28		57	71	3.6	1230
VCR Series-Parallel FHEV	3035	3.8	23	14	100	84		1235

The results of fuel consumption in the WLTC for the optimum cases (Figure 15) show that the VCR system allows a decrease in the fuel consumption of 3.3% with respect to the fixed CR. As was seen in Figure 3b, the high CR at low load improves the ICE efficiency. In spite of having engine map zones with BSFC improvements higher than 5%, in transient conditions the overall benefits are lower due to working in a greater area. Moreover, the hybridization of the powertrain plus the VCR system shows higher benefits in terms of fuel consumption. The application of a low electrification level

allows an improvement of 7.7% with respect to the no-hybrid fixed CR. However, the full electrification level improves even more the results, with benefits over 15% for the three different powertrains architectures. The best results were found for the series-parallel powertrain due to the flexibility of having the advantage to operate as a series in low vehicle speeds and as parallel at high speeds (over 92 km/h). In spite of the better results for the series-parallel, the P2 FHEV shows similar fuel consumption values. Therefore, the increase in the powertrain layout complexity seems to not compensate the fuel benefits. In this context, it is possible to affirm that the P2 FHEV is the best configuration in terms of hybrid complexity and fuel reduction.

Figure 16 shows an energy analysis for each powertrain along the WLTC. This graph allows to detect the losses due to each powertrain component, which complements the results obtained in the fuel consumption graph. Figure 16a shows that the VCR system and the hybridization of the powertrain reduce the ICE losses. As the total amount of energy required to perform the cycle is not constant due to variations in the vehicle weight and mechanical losses, the ICE efficiency in percentage was added in Figure 16b. The series mode allows improvements in the ICE efficiency by avoiding its transient operation. The total benefits by using both technologies (VCR + Hybrid) is around 7% in terms of ICE operative thermal efficiency.

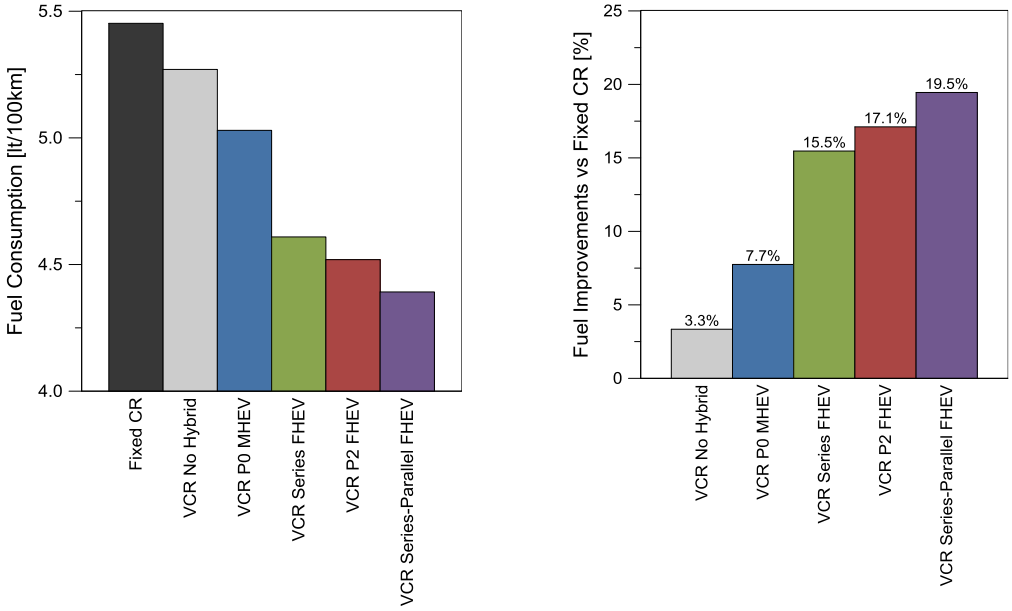

(a) (b)

Figure 15 – Fuel consumption for VCR hybrid vehicles in absolute value (a) and comparative to the no-hybrid fixed CR (b).

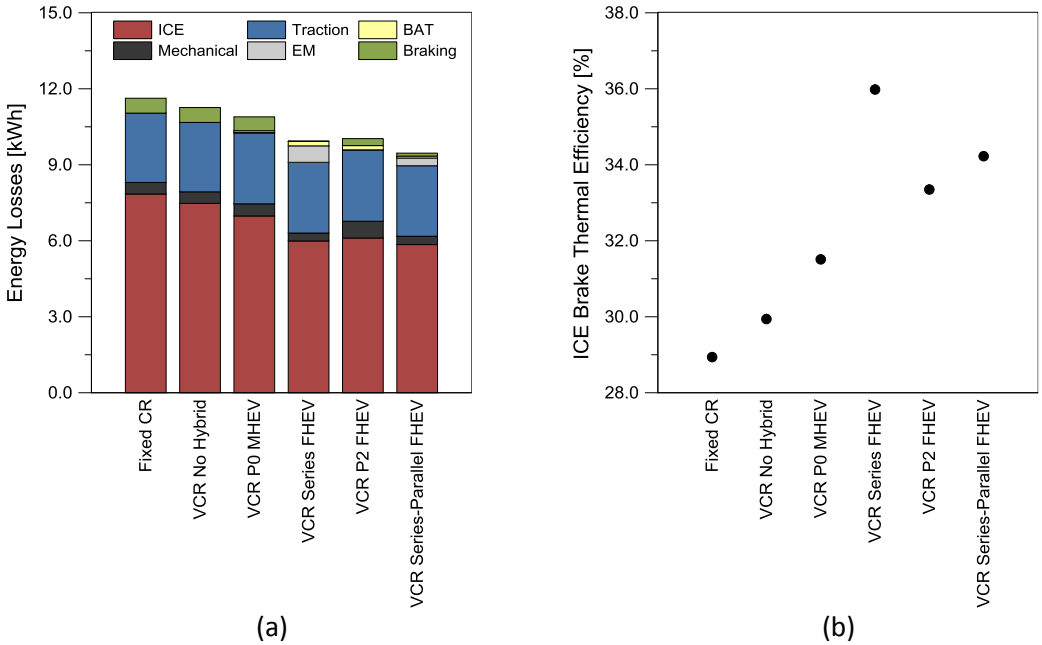

(a) (b)

Figure 16 – Energy losses (a) and ICE thermal efficiency (b) for VCR hybrid, no-hybrid and fixed CR vehicles.

Following the performance analysis, the engine-out NOx emissions levels are far from those required to pass the Euro 6 emission legislation (0.06 g/km) for all the vehicle platforms, as shown in the previous section. Thus, an after-treatment device as a TWC is necessary to achieve the tail-pipe target values. Moreover, Figure 17 shows that the VCR operation allows improvements in NOx up to 6%. On the other hand, the results when the vehicle is electrified does not show clear advantages to reduce NOx emissions. Figure 18 shows the results in terms of particle number emissions. In spite the VCR applied in a no-hybrid powertrain increase the PN emissions, the hybridization allows to strongly reduce the levels of this parameter. All the FHEV technologies are under Euro 6 limit. This is mainly because of the use of better engine map zones that in a conventional powertrain. In this sense, the series mode is the best solution, with a reduction of 60% the PN emissions, operation closer to the highest efficiency zone.

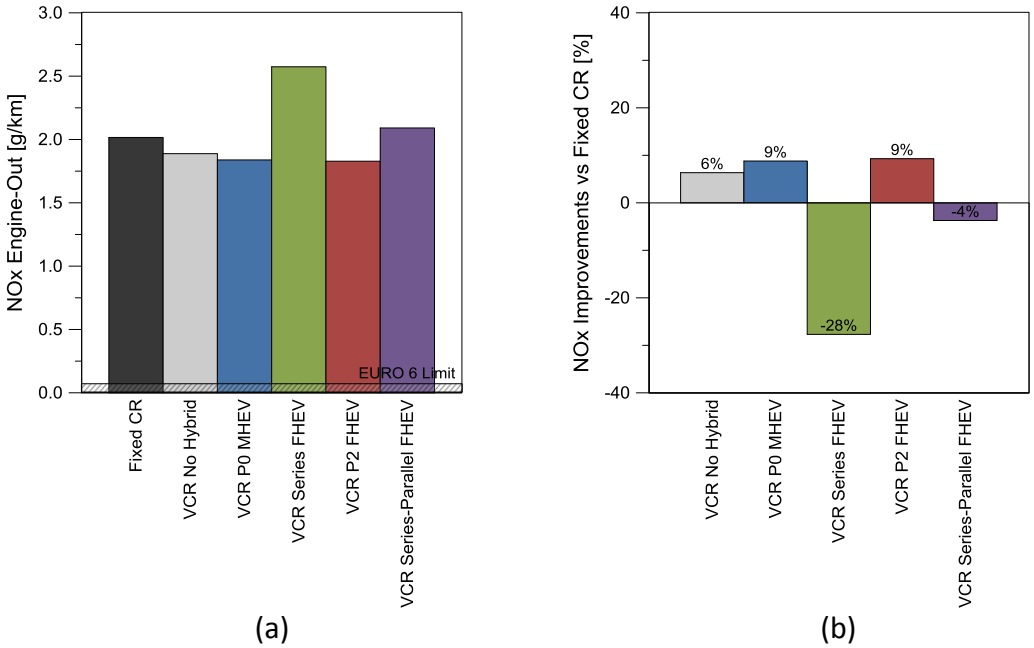

Figure 17 – NOx engine-out emissions for VCR hybrid vehicles in absolute value (a) and comparative to the fixed CR (b).

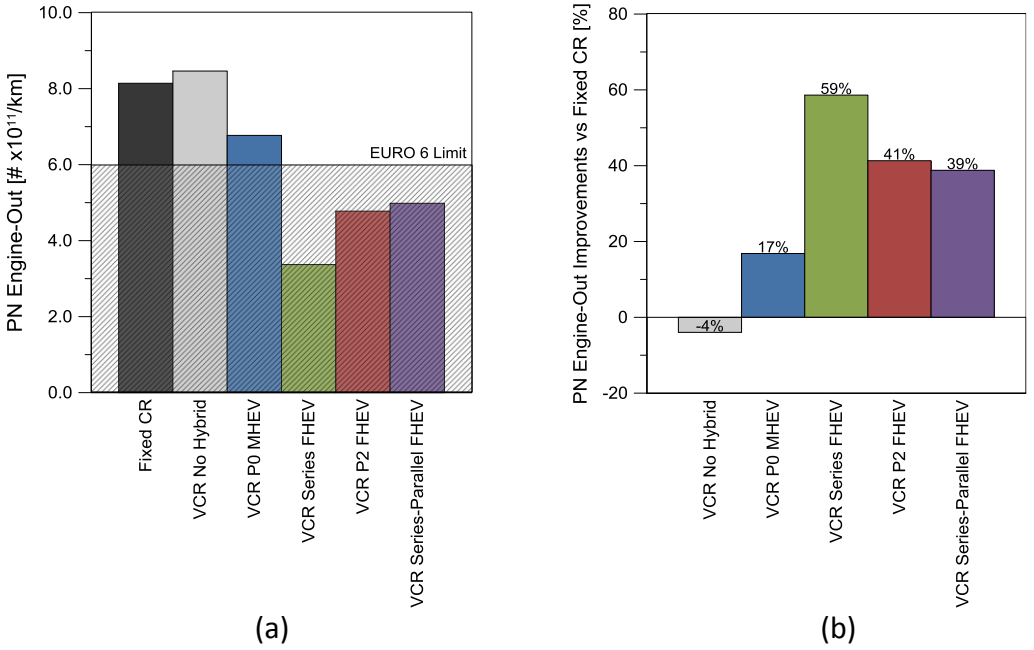

Figure 18 – Particle number (PN) engine-out emissions for VCR hybrid vehicles in absolute value (a) and comparative to the fixed CR (b).

In terms of CO and HC (Figure 19), the results show some improvements using hybrid technologies but are not enough to achieve the Euro 6 legislation. In addition, the VCR does not show benefits in these two pollutants. As in the case of NOx, a TWC it is necessary to achieve the target Euro 6 values. The engine-out CO_2 results (Figure 20) show similar trend than the fuel consumption (Figure 15). As it is well known, the emission of this component is proportional to the fuel consumption mass with the carbon mass ratio. However, in gasoline engines the CO and HC are none negligible. Therefore, the relation is not maintained at engine-out. For this reason, the P2 (highest

CO emissions) suffers a high decrease in the CO_2 emissions. The European Parliament set a CO_2 target for 2021 of 95 g/km (dashed box) to reduce the global world pollution. In spite of the full hybrid is closer or below this target, are not measured at tailpipe as required by the legislation. Therefore, the values need to be analyzed carefully. To complement this analysis, the calculated CO_2 tailpipe emissions from a stoichiometric combustion are shown in Figure 21. The calculus was performed considering the fuel mass consumption results and the carbon content of the gasoline (Table 2). The results show that series-parallel FHEV allows the lowest CO_2 emission (102 g/km). However, the desired 2021 target was not achieved and further improvements need to be done (7 g/km of CO_2). Between the possible improvements are the re-calibration of the VCR engine map to operate in a hybrid powertrain, the reduction of vehicle weight by using advanced vehicle materials and the use of low resistance tires, among others.

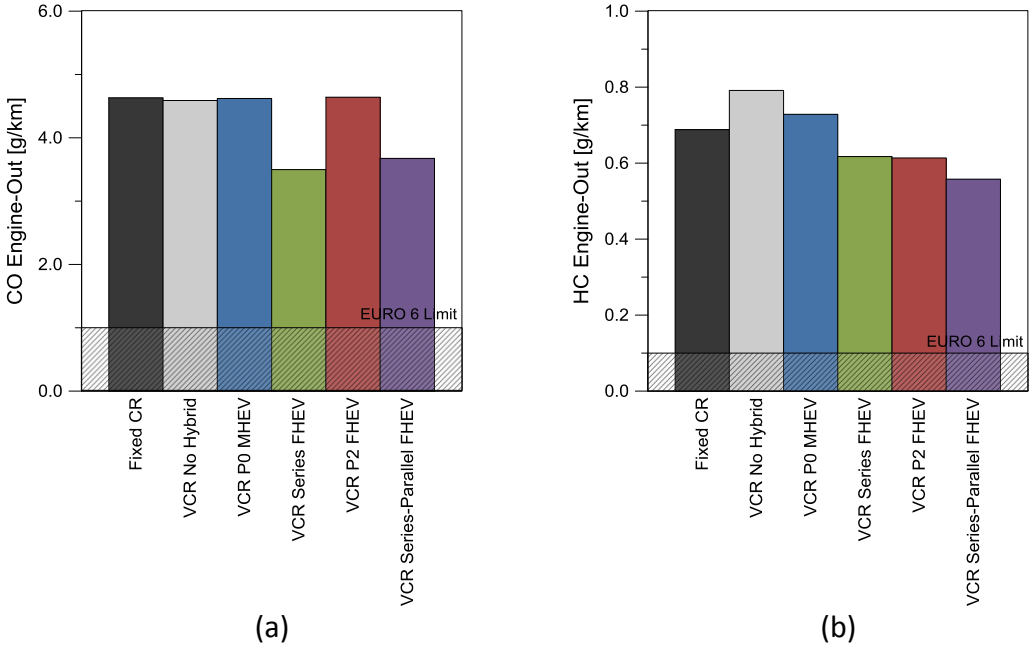

Figure 19 – CO (a) and HC (b) engine-out emissions for VCR hybrid and no-hybrid vehicle and the fixed CR no-hybrid vehicle.

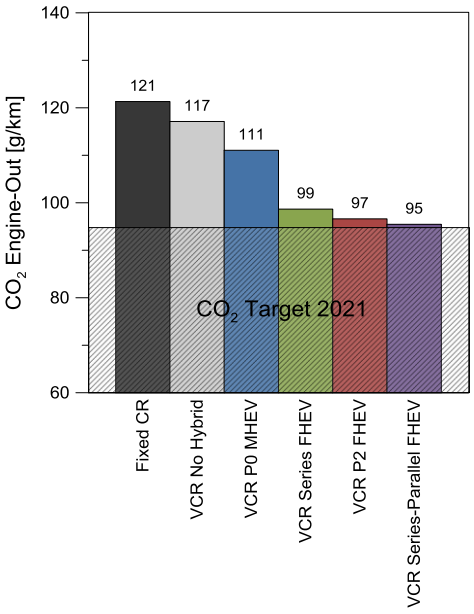

Figure 20 – CO_2 engine-out emissions for VCR hybrid and no-hybrid vehicle and the fixed CR no-hybrid vehicle.

As was mentioned before, the CO, HC and NOx need to be reduced to achieve the Euro 6 at the tailpipe. In commercial applications, the three-way catalyst (TWC) is considered the best solution for gasoline engines due to the reduction of the three components with a unique system of relative low cost. The main requirement is the use of a narrow range of the equivalence ratio for which the single-bed three-way unit is effective in controlling all three emissions. Therefore, to have high efficiency (over 85%) [38] it requires a precise metering of the fuel mass concentration at each instant. For this, a similar approach that was used in the engine test bench is applied in the vehicle to the close-loop control system that uses an oxygen sensor located in the exhaust stream. Figure 21 shows an analysis of the results obtained in terms of the engine-out emissions and the required global efficiency that is necessary in the TWC and the GPF to achieve the Euro 6 targets. The efficiency is calculated trough the $Emissions_{Engine-out}/Emission_{Euro\ 6\ limit}$ ratio. In spite of the variations in the pollutant emissions showed in this section, the ATS requirements, especially in the TWC, are closer to that needed in a conventional no-hybrid fixed CR vehicle. This means that a similar TWC could be used to reduce the three pollutant emissions in terms of capacity and global efficiency.

Gasoline particle filters (GPFs) are necessary to meet the particle number (PN) emission standards for direct injection gasoline passenger cars. Figure 21 shows that for the full hybrid vehicles this ATS is not necessary, giving great advantages to this technology. Also, the MHEV allows a high decrease of the GDF use, reducing the regeneration times required and the complexity of the system.

In addition to the air fuel ratio control, the reactions depend on the temperature of the internal surfaces of the converter. The light-off temperature at which the reactions start is around 300 °C, while the highest conversion rate requires temperatures in the 400–700 °C range. This is a critical point in hybrid vehicles due to the several turn -on and -off of the ICE. Therefore, a deeper analysis needs to be performed in the future to see the thermal behavior of the TWC in hybrid platforms.

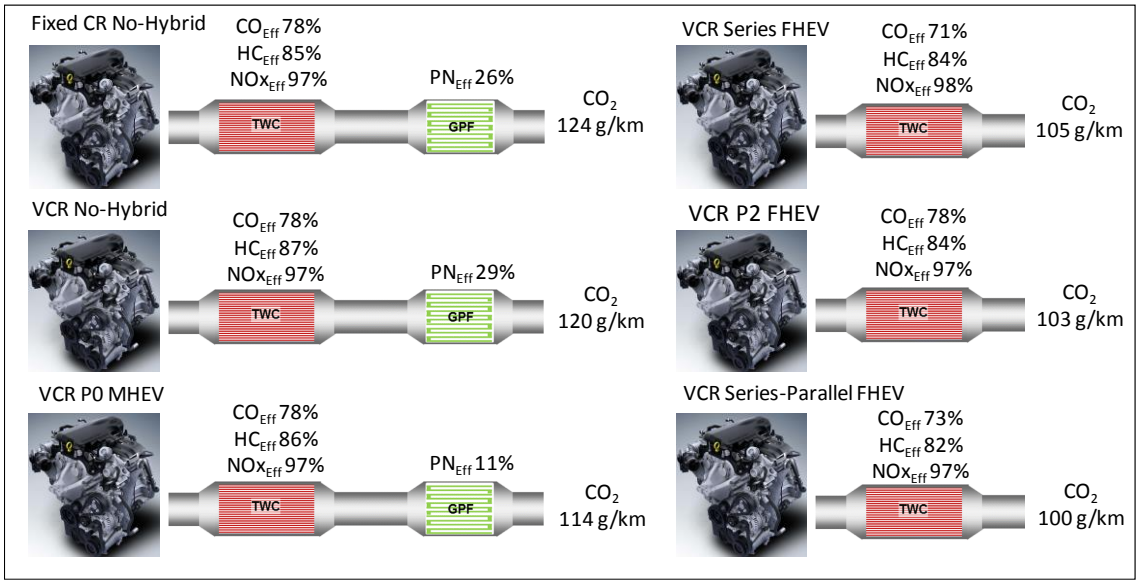

Figure 21 – After Treatment System necessary for No-Hybrid and Hybrid VCR ICE with respect to the no-hybrid fixed CR vehicle.

3.1.3. Hybrid Powertrain behavior under RDE

The discrepancy between the NEDC, more realistic dynamometer driving cycles, and real-life cycles got evident as soon as tests were performed with portable emissions measurement systems (PEMS). RDE testing will force to bring down the real-world driving emissions by passenger cars significantly. It was considered a CF of 1.43 (0.089 g/km) and CF of 1.5 for PN ($9x10^{11}$ #/km) as the normative impose up to 2025.

Figure 22 shows a similar trend in the RDE cycle than the observed in the WLTC (Figure 15) with the VCR system improving the fuel consumption versus the fixed CR and the hybrid platforms gaining extra benefits. In addition, higher benefit was seen for the series-parallel FHEV than the P2 FHEV. The results suggest that the possibility to use two different modes (series and parallel operation) in real life cycles improves the vehicle performance. Another important result is the increase of the fuel consumption in the RDE as compared to the WLTC, with around 10% for no-hybrid platforms and 3%-7% for hybrid platforms. The main reasons are the presence of a larger urban zone and the altitude of the road. In addition, the emissions were also increased as declared in several previous works found in the literature [39,40]. The NOx emissions are still far from the legislation targets, with values over 1.5 g/km being the lowest again the P2 FHEV. On the other hand, as the PN limit increase, it is possible to see that all the hybrid vehicles are inside the CF limits (red dashed box) including the P0 MHEV.

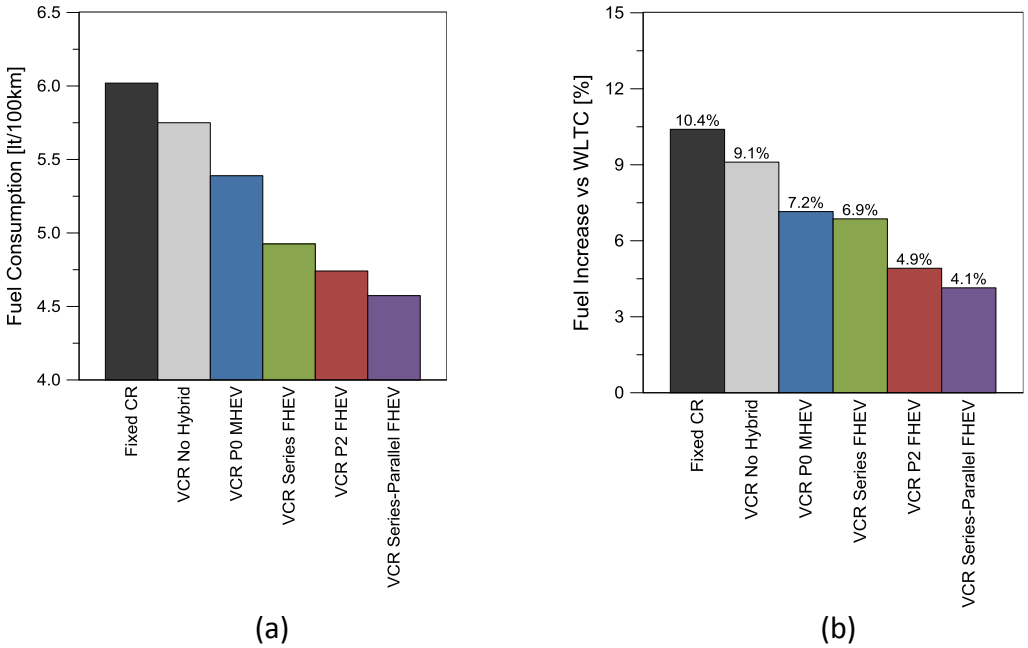

Figure 22 – After Treatment System necessary for No-Hybrid and Hybrid VCR ICE with respect to the no-hybrid fixed CR vehicle.

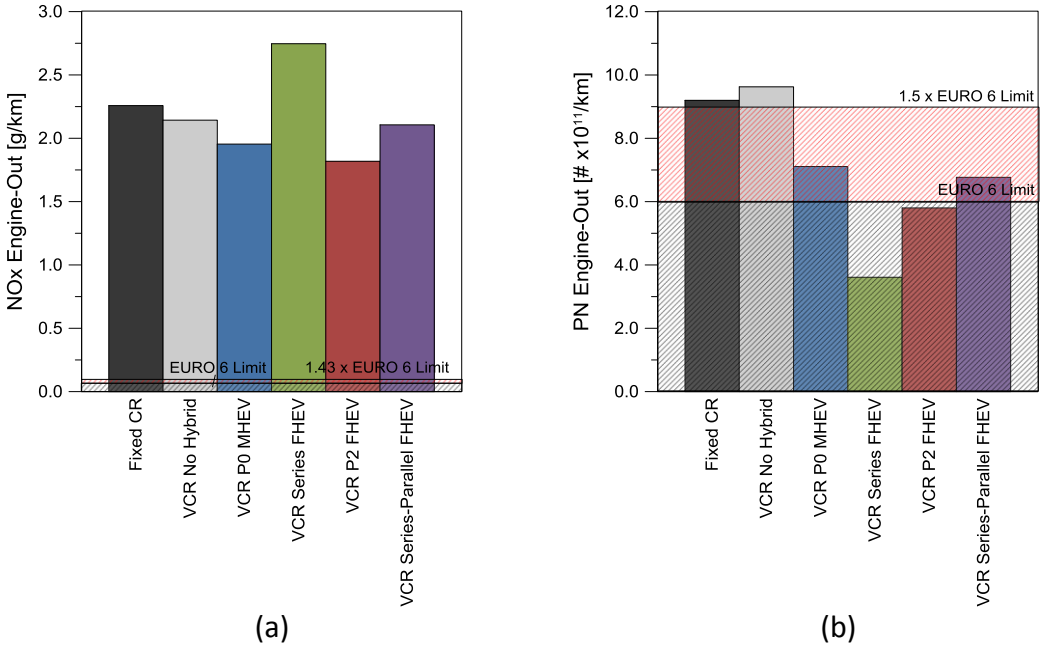

Figure 23 – After Treatment System necessary for No-Hybrid and Hybrid VCR ICE with respect to the no-hybrid fixed CR vehicle.

4. Conclusions

This work investigated the potential of implementing the VCR technology in several hybrid electric vehicles platforms. The results are compared against a traditional fixed compression ratio engine. Moreover, all the study was done under the current European normative (WLTP) that contemplates conventional and hybrid vehicles. From this study, it was found that:

- The VCR system allows fuel improvements of 3% in conventional powertrains, 8% in Mild and 17% in full hybrid powertrains. The electrification level (MHEV vs

FHEV) was seen more determinant than the powertrain architecture (P0, P2, series and series-parallel). The P2 and series-parallel were seen the most effective to achieve low fuel consumption and emissions (NOx and Soot).

- The energy analysis shows that the main losses are in the ICE instead in the other powertrain components. However, the hybridization combined with VCR system allows improvements from 29% to 36% in the ICE brake efficiency. The regenerative braking is other source of energy that allows the improvements in fuel consumption for hybrid vehicles.
- For NOx, HC and CO, the three-way catalytic is still necessary to achieve the string Euro 6 legislation. However, the hybridization allows to avoid the use of the gasoline particle filter due to engine particle number below $6x10^{11}$ #/km.
- In spite of the large improvements in CO_2 emissions, the tailpipe estimations are over the Euro 6 requirements. Therefore, other technology needs to be applied to achieve 2021 CO_2 targets.
- The RDE test of the no-hybrid and hybrid VCR vehicles shows an increase of the fuel consumption and emissions with respect to the WLTC. However, the results were better for hybrid than no-hybrid vehicles. The no-hybrid increases in 10%, instead the series-parallel FHEV that was only 2.4% in fuel consumption. In addition, the PN was below CF soot limits for all hybrid vehicles.

The results show that hybrid technology together with VCR system has strong potential to reduce local and global pollution. However, it is important to note that the advance system and re-calibration of the ICE to operate with hybrid powertrains need to be applied to achieve the future CO_2 targets.

Acknowledgments

The authors acknowledge FEDER and Spanish Ministerio de Economía y Competitividad for partially supporting this research through TRANCO project (TRA2017-87694-R). The authors also acknowledge the Universitat Politècnica de València for partially supporting this research through Convocatoria de ayudas a Primeros Proyectos de Investigación (PAID-06-18).

References

[1] González RM, Marrero GA, Rodríguez-López J, Marrero ÁS. Analyzing CO 2 emissions from passenger cars in Europe: A dynamic panel data approach. Energy Policy 2019;129:1271–81. doi:10.1016/j.enpol.2019.03.031.

[2] Commission Regulation Europe. Setting emission performance standards for new passenger cars as part of the Community's integrated approach to reduce CO2 emissions from light-duty vehicles. 2009. doi:http://eur-lex.europa.eu/pri/en/oj/dat/2003/l_285/l_28520031101en00330037.pdf.

[3] Dua R, White K, Lindland R. Understanding potential for battery electric vehicle adoption using large-scale consumer profile data. Energy Reports 2019;5:515–24. doi:10.1016/j.egyr.2019.04.013.

[4] Luján JM, Bermúdez V, Dolz V, Monsalve-Serrano J. An assessment of the real-

world driving gaseous emissions from a Euro 6 light-duty diesel vehicle using a portable emissions measurement system (PEMS). Atmos Environ 2018;174:112–21. doi:10.1016/j.atmosenv.2017.11.056.

[5] Fayad MA, Fernández-Rodríguez D, Herreros JM, Lapuerta M, Tsolakis A. Interactions between aftertreatment systems architecture and combustion of oxygenated fuels for improved low temperature catalysts activity. Fuel 2018;229:189–97. doi:10.1016/j.fuel.2018.05.002.

[6] Benajes J, García A, Monsalve-Serrano J, Boronat V. Dual-Fuel Combustion for Future Clean and Efficient Compression Ignition Engines. Appl Sci 2016;7:36. doi:10.3390/app7010036.

[7] Lanzarotto D, Marchesoni M, Passalacqua M, Prato AP, Repetto M. Overview of different hybrid vehicle architectures. IFAC-PapersOnLine 2018;51:218–22. doi:10.1016/j.ifacol.2018.07.036.

[8] Lemazurier L, Shidore N, Kim N, Moawad A, Rousseau A, Bonkoski P, et al. Impact of Advanced Engine and Powertrain Technologies on Engine Operation and Fuel Consumption for Future Vehicles. SAE Int., 2015. doi:10.4271/2015-01-0978.

[9] Pasini G, Lutzemberger G, Frigo S, Marelli S, Ceraolo M, Gentili R, et al. Evaluation of an electric turbo compound system for SI engines: A numerical approach. Appl Energy 2016;162:527–40. doi:10.1016/j.apenergy.2015.10.143.

[10] Zhou X, Qin D, Hu J. Multi-objective optimization design and performance evaluation for plug-in hybrid electric vehicle powertrains. Appl Energy 2017;208:1608–25. doi:10.1016/j.apenergy.2017.08.201.

[11] Benajes J, García A, Monsalve-Serrano J, Martínez-Boggio S. Emissions reduction from passenger cars with RCCI plug-in hybrid electric vehicle technology. Appl Therm Eng 2020;164:114430. doi:10.1016/j.applthermaleng.2019.114430.

[12] Asghar M, Bhatti AI, Ahmed Q, Murtaza G. Energy Management Strategy for Atkinson Cycle Engine Based Parallel Hybrid Electric Vehicle. IEEE Access 2018;6:28008–18. doi:10.1109/ACCESS.2018.2835395.

[13] Solouk A, Shakiba-herfeh M, Shahbakhti M. Analysis and Control of a Torque Blended Hybrid Electric Powertrain with a Multi-Mode LTC-SI Engine. SAE Int J Altern Powertrains 2017;6:2017-01–1153. doi:10.4271/2017-01-1153.

[14] Wang C, Zhang F, Wang E, Yu C, Gao H, Liu B, et al. Experimental study on knock suppression of spark-ignition engine fuelled with kerosene via water injection. Appl Energy 2019;242:248–59. doi:10.1016/j.apenergy.2019.03.123.

[15] Teodosio L, Pirrello D, Berni F, De Bellis V, Lanzafame R, D'Adamo A. Impact of intake valve strategies on fuel consumption and knock tendency of a spark ignition engine. Appl Energy 2018;216:91–104. doi:10.1016/j.apenergy.2018.02.032.

[16] Wolfgang S, Sorger H, Loesch S, Unzeitig W, Huettner T, Fuerhapter A. The 2-Step VCR Conrod System - Modular System for High Efficiency and Reduced CO2.

SAE Tech Pap Ser 2017;1. doi:10.4271/2017-01-0634.

[17] Shaik A, Moorthi NSV, Rudramoorthy R. Variable compression ratio engine: A future power plant for automobiles - an overview. Proc Inst Mech Eng Part D J Automob Eng 2007;221:1159–68. doi:10.1243/09544070JAUTO573.

[18] Wittek K, Geiger F, Andert J, Martins M, Cogo V, Lanzanova T. Experimental investigation of a variable compression ratio system applied to a gasoline passenger car engine. Energy Convers Manag 2019;183:753–63. doi:10.1016/j.enconman.2019.01.037.

[19] Kleeberg H, Tomazic D, Dohmen J, Wittek K, Balazs A. Increasing Efficiency in Gasoline Powertrains with a Two-Stage Variable Compression Ratio (VCR) System. SAE Tech Pap Ser 2013;1. doi:10.4271/2013-01-0288.

[20] Teodosio L, De Bellis V, Bozza F, Tufano D. Numerical Study of the Potential of a Variable Compression Ratio Concept Applied to a Downsized Turbocharged VVA Spark Ignition Engine. SAE Tech Pap Ser 2017;1. doi:10.4271/2017-24-0015.

[21] Morra E, Spessa E, Ciaravino C, Vassallo A. Analysis of Various Operating Strategies for a Parallel-Hybrid Diesel Powertrain with a Belt Alternator Starter. SAE Int J Altern Powertrains 2012;1:2012-01–1008. doi:10.4271/2012-01-1008.

[22] Fahrzeug- AK, Vassallo A, Cipolla G, Mallamo F, Paladini V, Powertrain GM, et al. Transient Correction of Diesel Engine Steady- State Emissions and Fuel Consumption Maps for Vehicle Performance Simulation. Aachener Kolloquium Fahrzeug- und Mot., 2007.

[23] Luján JM, García A, Monsalve-Serrano J, Martínez-Boggio S. Effectiveness of hybrid powertrains to reduce the fuel consumption and NOx emissions of a Euro 6d-temp diesel engine under real-life driving conditions. Energy Convers Manag 2019;199:111987. doi:10.1016/j.enconman.2019.111987.

[24] Pasquier M, Duoba M, Rousseau A. Validating Simulation Tools for Vehicle System Studies Using Advanced Control and Testing Procedure 2014.

[25] Benajes J, García A, Monsalve-Serrano J, Martínez-Boggio S. Optimization of the parallel and mild hybrid vehicle platforms operating under conventional and advanced combustion modes. Energy Convers Manag 2019;190:73–90. doi:10.1016/j.enconman.2019.04.010.

[26] Morra E, Spessa E, Ciaravino C, Vassallo A. Analysis of Energy-Efficient Management of a Light-Duty Parallel-Hybrid Diesel Powertrain with a Belt Alternator Starter. SAE Int J Altern Powertrains 2012;1:2012-01–1008. doi:10.4271/2011-24-0080.

[27] Huo Y, Yan F, Feng D. A hybrid electric vehicle energy optimization strategy by using fueling control in diesel engines. Proc Inst Mech Eng Part D J Automob Eng 2019;233:517–30. doi:10.1177/0954407017747372.

[28] Liu Z, Ivanco A, Filipi ZS. Impacts of Real-World Driving and Driver Aggressiveness on Fuel Consumption of 48V Mild Hybrid Vehicle. SAE Int J Altern Powertrains 2016;5:2016-01–1166. doi:10.4271/2016-01-1166.

[29] Wang R, Yu W, Meng X. Performance investigation and energy optimization of a thermoelectric generator for a mild hybrid vehicle. Energy 2018;162:1016–28. doi:10.1016/j.energy.2018.08.103.

[30] Solouk A, Shakiba-Herfeh M, Arora J, Shahbakhti M. Fuel consumption assessment of an electrified powertrain with a multi-mode high-efficiency engine in various levels of hybridization. Energy Convers Manag 2018;155:100–15. doi:10.1016/j.enconman.2017.10.073.

[31] Sarlioglu B, Morris CT, Han D, Li S. Benchmarking of electric and hybrid vehicle electric machines, power electronics, and batteries. 2015 Intl Aegean Conf. Electr. Mach. Power Electron., IEEE; 2015, p. 519–26. doi:10.1109/OPTIM.2015.7426993.

[32] Rouhani A, Kord H, Mehrabi M. A comprehensive method for optimum sizing of hybrid energy systems using intelligence evolutionary algorithms. Indian J Sci Technol 2013;6:4702–12. doi:10.1016/j.enconman.2010.09.028.

[33] Olivier J, Peters J. Trends in global CO2 and total greenhouse gas 2018 report. 2018.

[34] Varella R, Giechaskiel B, Sousa L, Duarte G. Comparison of Portable Emissions Measurement Systems (PEMS) with Laboratory Grade Equipment. Appl Sci 2018;8:1633. doi:10.3390/app8091633.

[35] Hochmann G, Berger A, Mayrhofer H. Achieving Compliance to RDE - How Does This Development Target Impact the Development Process, Testing Methodologies and Tools. Symp. Int. Automot. Technol. 2019, SAE International; 2019. doi:https://doi.org/10.4271/2019-26-0358.

[36] Registry G. Global technical regulation No. 15. Glob Regist 2017;14568:87.

[37] Shields MD, Zhang J. The generalization of Latin hypercube sampling. Reliab Eng Syst Saf 2016;148:96–108. doi:10.1016/j.ress.2015.12.002.

[38] Kašpar J, Fornasiero P, Hickey N. Automotive: catalytic converters current status. Catal Today 2003;77:419–49. doi:10.1016/S0920-5861(02)00384-X.

[39] Favre C, Bosteels D, May J. Exhaust Emissions from European Market-Available Passenger Cars Evaluated on Various Drive Cycles. SAE Tech Pap Ser 2013;1. doi:10.4271/2013-24-0154.

[40] Pavlovic J, Ciuffo B, Fontaras G, Valverde V, Marotta A. How much difference in type-approval CO2 emissions from passenger cars in Europe can be expected from changing to the new test procedure (NEDC vs. WLTP)? Transp Res Part A Policy Pract 2018;111:136–47. doi:10.1016/j.tra.2018.02.002.

[41] García A, Monsalve-Serrano J, Sari R, Dimitrakopoulos N, Tunér M, Tunestål P. Performance and emissions of a series hybrid vehicle powered by a gasoline partially premixed combustion engine. Appl Therm Eng 2019;150:564–75. doi:10.1016/j.applthermaleng.2019.01.035.

Abbreviations

ATS	Aftertreatment sytems
BEV	Battery electric vehicles
BMEP	Brake mean effective pressure
BSCO	Brake specific CO emissions
$BSCO_2$	Brake specific CO_2 emissions
BSFC	Brake specific fuel consumption
BSHC	Brake specific HC emissions
BSNOx	Brake specific NOx emissions
BSPN	Brake specific particle number emissions
CCW	Counter Clockwise
CW	Clockwise
CDC	Conventional diesel combustion
CI	Compression Ignition
CO	Carbon Monoxide
CR	Compression ratio
DI	Direct Injection
DISI	Direct Injection Spark Ignition Engine
DoE	Design of Experiments
DPM	Dynamic programming method
ECMS	Equivalent consumption minimization strategy
ECU	Engine control unit
EM	Electric motor
EU	European Union
FCV	fuel cell vehicles
FHEV	Full hybrid vehicle
GEN	Generator Motor
GHG	greenhouse gas emissions
GPF	Gasoline Particulate Filter
HC	Unburned Hydrocarbons
HEV	Hybrid electric vehicle
ICE	Internal combustion engine
LI-Ion	Litium Ion batteries
LTC	Low Temperature Combustion
MFB	Mass fraction burned
MHEV	Mild hybrid electric vehicle
NEDC	New European Driving Cycle
NOx	Nitrogen Oxides
OEM	Original equipment manufacturer
P0	Belt alternator starter hybrid powertrain
P2	Parallel hybrid electric vehicle
PHEV	Plug in electric vehicle
PM	particle matter
PN	Particle number
RBC	Rule base control
RCCI	Reactivity Controlled Compression Ignition
RDE	Real driving emission test
rpm	Revolution per minute
SI	Spark Ignition
SOC	State of the charge of the battery
TM	Traction Motor
TTW	Tank to wheel
TWC	Three way catalytic
VCR	Variable compression ratio
VVA	Variable valve actuation
WLTC	Worldwide Harmonized Light Vehicles Cycle
WLTP	Worldwide Harmonized Light Test Procedure
WTW	Well to wheel

Appendix A – Emissions ICE Maps

Emission maps for HC, CO and CO_2 measured at engine out for the VCR optimum CR selection are depicted in Figure A1 and Figure A2.

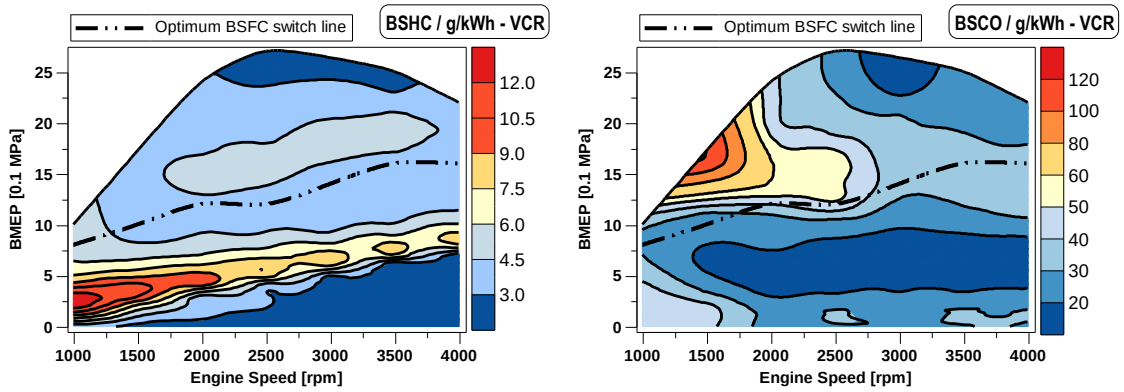

Figure A1 – VCR brake specific HC (a) and CO (b) engine-out emissions.

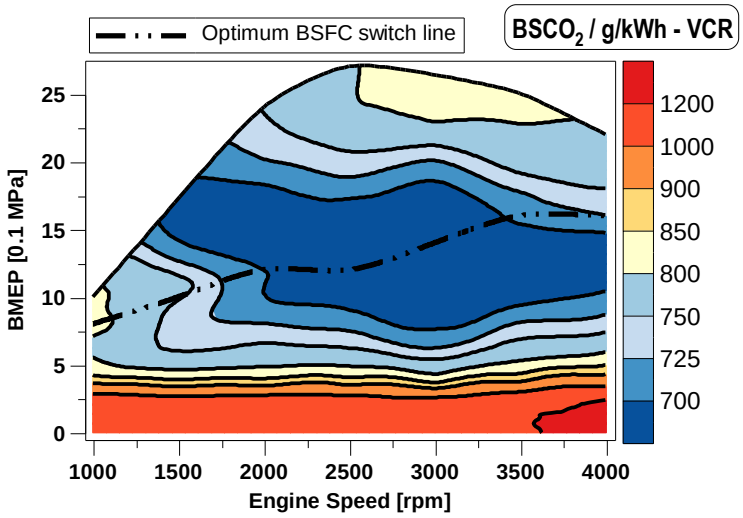

Figure A2 – VCR brake specific CO_2 engine-out emission.

Appendix B – Hybrid Control

A rule-based controller approach was used to determines the hybrid operative modes. This means that several predefine rules are set without taking in consideration the driving cycle. In spite of not been a global optimized strategy as dynamic programming method (DPM) or equivalent consumption minimization strategy (ECMS), it is extensively used due to the robust of the implementation. It is important to note that an initial state of the charge (SOC) of 0.64 was used.

Table B1 shows the vehicle modes with the respective ICE and electric motor requirements for P0 and P2 hybrid architectures. Table B2 shows the control for the series hybrid mode in which three level of charge were set.

Table B1 - Operation mode of Supervisory Controller for P0 HEV, P2 FHEV and Series-Parallel at high speed.

Vehicle State	Sub-state	ICE State	ICE Power Required	EM Power Required	Condition
EV*	Zero	Off	0	0	V=0 and $Brake_{Position}$=100%
	EV	Off	0	Driver	V < [V_{Limit}] & $Charge_{State}$=0
HEV - Vehicle Stop	ICE Start	Off	0	-$Start_{ICE}$	V=0 & $Charge_{State}$=1 & ICE_{Speed}<1000
	Idle Charging	On	Charge	-Charge	V=0 & $Charge_{State}$=1 & ICE_{Speed}>1000
HEV - Vehicle Moving and Accelerate	ICE Start	Off	0	Driver+$Start_{ICE}$	Driver>0 & V>[V_{Limit}] & ICE_{Speed}<1000
	Power Assist	On	[Split]*Driver	[Split]*Driver	Driver>0 & V>[V_{Limit}] & ICE_{Speed}>1000 & [Split]*Driver<EM_{max}
	Normal	On	Driver	0	Driver>0 & V>[V_{Limit}] & ICE_{Speed}>1000 & [Split]*Driver>EM_{max} & $Charge_{State}$=0
	Power Assist Max ICE	On	ICE_{max}	Driver-ICE_{max}	Driver>ICE_{maxT}
	Charging	On	Driver+Charge	-Charge	Driver>0 & ICE_{Speed}>1000 & $Charge_{State}$=1
HEV - Vehicle Moving and Braking	Regenerative Braking	Off	0	Driver	SOC<SOC_{max} & Driver>EM_{Min}
	Breaking Mixed	Off	0	EM_{min}	SOC<SOC_{max} & Driver < EM_{Min}
	No Regenerative Breaking	Off	0	0	SOC ≥ SOC_{max}

*Only for FHEV-P2, [x] DoE control parameters.

Table B2 - Operation mode of Supervisory Controller for Series and Series-Parallel (low speed) FHEV.

Vehicle State	Sub-state	ICE State	ICE Power Required	GEN Power Required	TM Power Required	Condition
Series	EV	Off	0	Driver	Driver	SOC ≥ SOC_{Level1}
	ICE Start	Off	0	-$Start_{ICE}$	Driver	SOC < SOC_{Level1} & ICE_{Speed} < 1000
	Level 1*	On	[GEN_{max}]/3	[GEN_{max}]/3	Driver	SOC < SOC_{Level1} & ICE_{Speed} > 1000
	Level 2*	On	2*[GEN_{max}]/3	2*[GEN_{max}]/3	Driver	SOC < SOC_{Level2}
	Level 3	On	[GEN_{max}]	[GEN_{max}]	Driver	SOC < SOC_{Level3}

*Only for Series FHEV, [x] DoE control parameters.